Department of Biosciences and Nutrition
Center for Biotechnology
Karolinska Institutet, Stockholm, Sweden

Protein Adaptability Involved in Self-Assembled Icosahedral Capsids

Josefina Nilsson

Karolinska Institutet

Stockholm 2006

Cover Illustration:
Cryo-EM three-dimensional reconstruction of the human polyomavirus BK VP1 virus-like particle.

Published and printed by Karolinska University Press
Box 200, SE-171 77 Stockholm, Sweden

ISBN 91-7140-717-0

ABSTRACT

Interactions between viral coat proteins determine the size and shape of the virus capsid. Therefore, the plain closed shell of a spherical virus provides an excellent resource for studying and testing protein–protein interactions. Recombinants systems can here be used to reveal the properties that lead to symmetrical capsids or other shapes. Icosahedral architecture similar to that found in viruses has also been adopted by some giant enzymes. In both, cases the biological activity and the shape of the particle are parameters that help to identify the accuracy of the small units forming the assembled giant molecule. *Vice versa*, the small units and their linkers may be engineered to guide the assembly into useful particles.

In this thesis, I focus on the protein framework in icosahedral virus-like particles of the human polyomavirus BK and the enzyme lumazine synthase from *Aquifex aeolicus*. My aim was to explore how a single type of building unit, in this case a pentamer, can assemble into particles with different size and surface morphology. This work includes the structure determination and comparison of two different virus-like particles (26.4 and 50.0 nm in diameter) of the human polyomavirus BK protein VP1. They both have icosahedral symmetry and their pentamic capsomers establish a T=1 and T=7d surface lattice, respectively. Likewise, the structure of a Lumazine synthase particle from *Aquifex aeolicus* was solved and compared to a previously solved structure of the native enzyme. The enzyme particle has a sequence insertion of four amino acids. This influences the shape of the assembly and the particles formed are approximately 14 nm larger in diameter than the native structure. The two systems, the virus-like particles and the enzyme particles, differ in their strategy for assembly: the BKV VP1 protein forms pentamers which are linked together by long (approximately 60 amino acids) flexible arms, while the enzyme protein is globular without protruding domains and uses relatively flat contact surfaces within pentamers and surrounding subunits. The BK virus-like particles primarily use the two loops, before and after the C-terminal helix, to adjust the position of the flexible arm. By that mean intercapsomer interactions can be kept as similar as possible even at different symmetrical environments and particle curvatures. In the case of the enzyme, the flexibility is not the result of different folding of a contact arm. Instead, alternative areas of the protein surface are used to form the interaction.

In all the particles studied, the hydrophobic effect seems to be a main stabilizing force. However, assembly of pentamers (or connecting subunits) also utilizes more specific interactions provided by patterns of complementary charges. Assembly of the “correct” quaternary structure in both systems may be driven by prosthetic groups. In the enzyme case flexibility is required for catalytic reasons - the active site is located at the subunit interface within the pentamer. Here the prosthetic group would control the needed motion for binding substrates and releasing products. In the case of the BK virus-like particles, the main flexibility is found within the C-terminal arm, forming the main interpentameric contacts. Here we find the assembly-controlling calcium ion. The electrostatic interactions and the prosthetic groups are placed in the structure for two functional purposes: to guide the assembly pathway and to maintain the local flexibility needed for assigned functions.

LIST OF PUBLICATIONS

This thesis is based on the following papers, which will be referred to in the text by their Roman numerals (I-IV).

I. Li, TC., Takeda, N., Kato, K., Nilsson, J., Xing, L., Haag, L., Cheng, R. H. and Miyamura T. (2003). Characterization of Self-Assembled Virus-like Particles of Human Polyomavirus BK Generated by Recombinant Baculoviruses. *Virology*, 311:115–124.

II. Nilsson, J., Miyazaki, N., Xing, L., Wu, B., Hammar, L., Li, TC., Takeda, N., Miyamura T. and Cheng, R. H. (2005). Structure and Assembly of a *T*=1 Virus-like Particle in BK Polyomavirus. *J. Virol.*, 79(9):5337-5345.

III. Nilsson, J., Xing, L., Zhang, X., Bergman, L., Haase, I., Fischer, M., Bacher, A., Meining, W., Ladenstein R. and Cheng, R. H. (2006). A 180 subunit complex of a lumazine synthase mutant violates quasi-equivalence in capsid assembly. *Manuscript*

IV. Nilsson, J., Aungsumart, S., Xing, L., Hammar, L., Li, TC., Takeda, N., Miyamura, T. and Cheng, R. H. The essential role of VP1 C-terminal arm in polyomavirus BK assembly and DNA incorporation. *Manuscript*

CONTENTS

LIST OF ABBREVIATIONS

3D	Three-dimensional
BKV	BK virus
cryo-EM	Electron cryomicroscopy
DNA	Deoxyribonucleic acid
IDEA	Sequence of Ile-Glu-Asp-Ala
JCV	JC virus
LS	Lumazine synthase
LSAQ	Lumazine synthase from *Aquifex aeolicus*
LSAQ-IDEA	Mutant of lumazine synthase from *Aquifex aeolicus* with the IDEA insertion
LSBS	Lumazine synthase from *Bacillus subtilis*
NLS	Nuclear localization signal
PFT	Polar fourier transform
RS	Riboflavin synthase
SV40	Simian virus 40
T	Triangulation number
VLPs	Virus-like particles
wt	Wild type
Å	Ångström (0.1 nm)

1 INTRODUCTION

1.1 OLIGOMERIC PROTEINS

Oligomeric proteins are composed of more than one subunit. The association of proteins into a quaternary structure, with a few subunits, and into even higher oligomers derives from the same types of interactions that define their tertiary folding. As with tertiary structures within the subunit, the bonds involved in holding the subunits together can be electrostatic interactions, van der Waals interactions, hydrogen bonds, hydrophobic effects and may even comprise reversible covalent bonds such as disulfide bonds, usually confined to formation of the secondary structure. The quaternary structure of the oligomeric assembly may include prosthetic groups or cofactors such as a specific metal ion which stabilize the assembly.

The evolution of oligomeric proteins is bounded by two opposing factors. On one hand there is an evolutionary trend toward large proteins to accommodate the selectivity of more specific functions. On the other hand, the mechanisms of protein synthesis, with its risk for mistakes, serve to limit the length of polypeptide chains and to favor smaller proteins over larger ones when high accuracy is needed. The typical mass of 30,000–50,000 Daltons is a compromise between these opposing forces (Srere, 1984). There are many examples of non-identical subunits that associate to form dimers, tetramers or even larger heteromeric units, which further oligomerize into giant macromolecular constructs, named heterologous oligomers. However, many oligomeric proteins are constructed from multiple copies of identical monomers. These are called homo-oligomers. Several reasons have been proposed for why homo-oligomers are favored in nature:

- *Error control* By building a large complex from many small subunits, translation errors may be reduced, and less material is lost by discarding subunits with defects. The fit of the small subunits into the final assembly also provides an extra level for proofreading (Kurland, 1992; Parker, 1989).
- *Coding efficiency* Homo-oligomers provide a genetically compact way to encode the information needed to build a large protein complex. Association of many copies of small subunits allows the creation of a large structure from a minimum of genetic space (Crick *et al.,* 1957).
- *Regulation of assembly* Large assemblies built of many identical subunits have attractive regulatory properties, because they are subjected to sensitive phase transitions (Monod, 1969).

1.1.1 Protein-protein interactions

Theories on structural features of protein-protein interfaces are presented in the work of Crane (1950). He concluded that the contact area or combined spots of two connecting proteins needs to be multiple and weak for a high degree of specificity. Furthermore,

the contact areas on one protein must have a complementary geometrical arrangement in the contact areas of the other protein.

The buried surface area in heterodimeric protein complexes have been found to be in the range 1200-4700 $Å^2$, where the majority of the examined protein complexes have a buried surface area of 1600 ± 400 $Å^2$ (Lo Conte *et al.,* 1999). The buried surface area in the dimeric interphase of homo-oligomeric complexes is usually larger, including examples where more than 9000 $Å^2$ is buried (Jones *et al.,* 1996). In this article, Jones *et al.* also show that homo-oligomeric complexes normally have a higher degree of curvature at the protein-protein interface than hetero-oligomers.

The relative importance of different bonds in oligomeric protein-protein interactions is still a matter of discussion. Enrichment of aromatic residues at the interface implies hydrophobic contributions, but there is often specific enrichment of arginines indicating that electrostatic interactions are also important (Stites, 1997; Lo Conte *et al.,* 1999). In the work by Larsen *et al.* the authors show that only one third of the 136 homodimeric proteins examined have a hydrophobic core at the protein-protein interface. Most of the homodimers are stabilized by a combination of small hydrophobic patches, polar interactions and a large number of bridging water molecules (Larsen *et al.,* 1998). The specificity requirements in protein-protein interactions might be one reason for the limited use of the hydrophobic effect as dominating interaction since they are less selective than salt-bridges and hydrogen bonds.

1.1.2 Structure and function

Protein oligomers have been selected by evolution to fit specific structural requirements, such as capacity to form rings, containers or filaments. The ability to adapt to conformational changes during assembly, genome release, or motion, is built into the quaternary structure, where the "correct" degree of stability/flexibility is crucial. The more stable domains are found in the internal core of each protein, or within the oligomeric substructure (dimer, trimer, pentamer …), while the more flexible parts are located at protein-protein interfaces. Such disordered segments might be functionally important in viral coat proteins, as reviewed by Liljas (2004). Sequences defining domains of functional value are as a general highly conserved. Variable domains are usually confined to the outer or inner surface of the particle shells, where patches of functional importance (like for instance receptor binding) usually remain constant during evolution. It is anticipated that the spherical arrangements of proteins favors icosahedral symmetry from minimum-energy reasons, but other shell arrangements are also known, when functionally more favorable.

1.2 ICOSAHEDRAL STRUCTURES AND THE THEORY OF QUASI-EQUIVALENCE

In their work from 1956, Crick and Watson pointed out that a viral genome is too small to provide enough genetic information for a polypeptide large enough to encapsidate it. They suggested that the viral capsid might be formed of multiple copies of one or a few proteins, which by repeated equivalent interactions assemble into symmetric closed

shells. This would then be large enough to enclose the genome (Crick *et al.,* 1956). In the years that followed negative contrasting of EM specimens was developed and applied to viruses (Brenner *et al.,* 1959). This opened a new era in virus research proving their oligomeric nature. The micrographs of spherical viruses, like the one of herpes virus by Wildy *et al.,* (1960), implied icosahedral arrangement of capsomers. This explained the 5-fold symmetry observed in the diffraction pattern of virus crystals that had confused the crystallographers of that time. The structural work that followed revealed that spherical capsids indeed display icosahedral symmetry (Finch *et al.,* 1959; Klug *et al.,* 1960), and thereafter, the discussion focused on the equivalence in local bonding and the total monomers allowed in a shell (for review see Morgan, 2004).

1.2.1 Icosahedral symmetry

A regular icosahedron is built of 20 triangular faces with 5-fold rotational symmetry at each of 12 vertices, 3-fold rotational symmetry at the center of each icosahedral face and 2-fold rotational symmetry in the middle of each edge (**Figure 1-1**). Each icosahedral face can be divided into three identical regions. Each of these 60 identical regions, all with symmetrically identical positions, is then referred to as an asymmetric unit, the basic building block of the icosahedral structure. Most viruses have capsids that are larger than can be created by 60 identical proteins in perfect icosahedral symmetry. Some viruses answer this need by creating capsids composed of several different subunits. For instance, poliovirus and rhinovirus capsids are composed of 60 copies of each of four different subunits, all arranged in perfect icosahedral symmetry. Other viruses take a more creative approach, using a single protein in several different quasi-equivalent structural environments. In these viruses, each of the 60 asymmetric units is filled by a number of copies of the same protein.

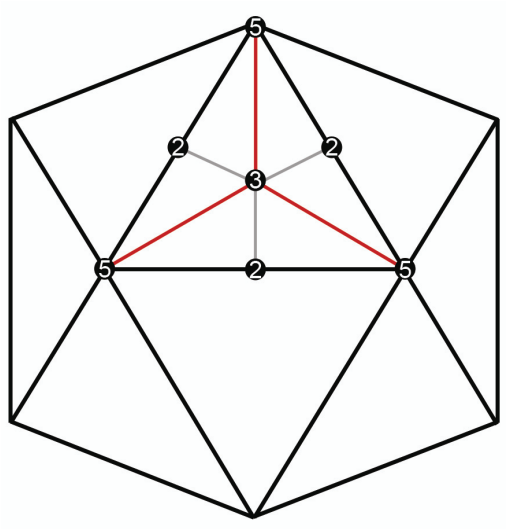

Figure 1-1: Schematic drawing of icosahedral symmetry. The positions of the symmetry axes are marked with the corresponding number (5, 3 and 2). The icosahedral face can be divided in different ways and still give rise to three identical asymmetric units, e.g., by connecting the three rotational symmetry axes (grey line) or two 5-folds and one 3-fold (red line).

1.2.2 The theory of quasi-equivalence

The quasi-equivalence theory of Caspar and Klug (1962) describes a model for how to assemble an icosahedral capsid containing more than 60 copies of one protein, *i.e.* more than one protein copy per asymmetric unit. They introduced the concept of triangulation of the asymmetric unit, *i.e.* the asymmetric unit was divided into equivalent sub-regions. The location of each sub-region in the icosahedron is not symmetrically equivalent; therefore, protein units located in that manner are located in similar fashion to each other, but not in equivalent positions. The basic hypothesis of the quasi-equivalence theory is that the bonds between the chemically identical units in the icosahedral virus capsid are of the same type. These bonds can be deformed to a certain degree to fit in the quasi-equivalent environments of the triangulated icosahedral structure. As stated by Klug: *"... if each subunit in the final structure still forms the same types or sets of bonds with its neighbors, then, although the units are no longer exactly equivalently related, they may be said to be quasi-equivalently related*" (Klug, 1969). The theory lead to the prediction that only certain multiples of 60 identical units are allowed, following the rule $T = h^2 + hk + k^2$, where h and k are integers and T is the triangulation number (**Figure 1-2**). The triangulation number defines the number of geometrically unique environments present in one asymmetric unit. Thus a T=3 icosahedral capsid contains 3 subunits in the asymmetric unit and the total number of subunits in the whole capsid is 60T, *i.e.,* 180 subunits.

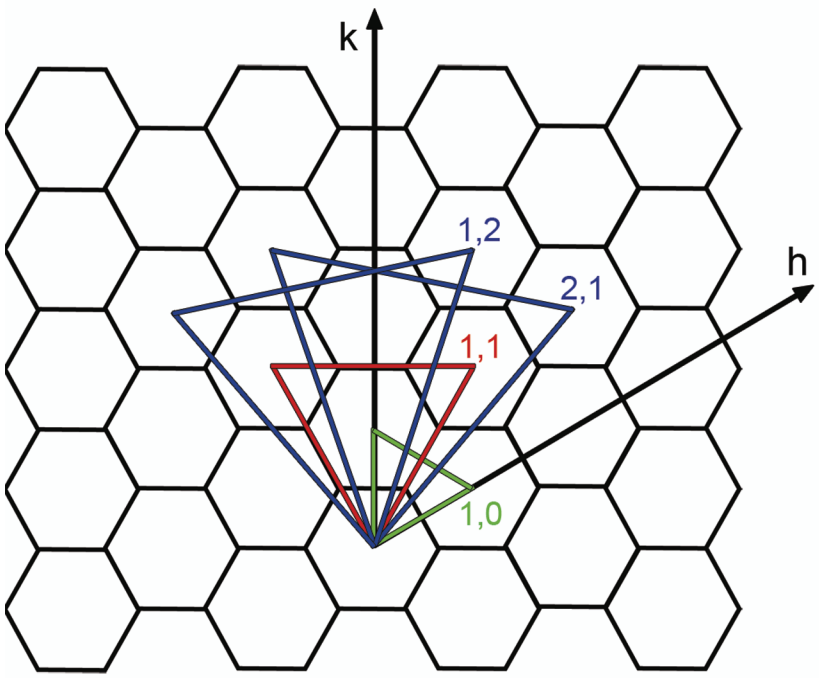

Figure 1-2: The construction of icosahedral capsids and their triangulation number. A closed icosahedral capsid can be formed when twelve hexamers are exchanged to pentamers in a hexagonal lattice. The positions at which hexamers are exchanged to pentamers can be defined by the integers h and k used to calculate the triangulation number. For example replacing hexamers with pentamers at position (1, 0) will give a T=1 capsid, replacement at (1, 1) produces a T=3 capsid and replacement at (2, 1) or (1, 2) yields capsids with T=7, indicated with green, red and blue, respectively.

1.2.2.1 The exceptions that confirms the rule…

There are, however, exceptions to the allowed *T* numbers where the capsid structures show a discrepancy in subunit numbers from the postulated 60*T* without violating the local equivalent contacts among subunits. For instance, polyomavirus has 360 subunits (instead of the expected 420) arranged into a *T*=7d surface lattice. In the polyomaviruses, the subunits assemble based on pentamer building-blocks throughout the entire icosahedral shell, where the pentamer rings occupy not only the pentameric positions but also the regular hexameric positions (Rayment *et al.,* 1982; Liddington *et al.,* 1991; Baker *et al.,* 1996; Stehle *et al.,* 1996; Li *et al.,* 2003). Likewise, the L-A virus was first reported to contain 120 subunits, resulting in a "*T* = 2" capsid which is a "not allowed" *T* number (Cheng *et al.,* 1994; Naitow *et al.,* 2002). Subsequent discoveries regarding the inner capsid organization of Blue tongue virus (BTV) and Rice dwarf virus (RDV) indicate that those capsids utilize a similar lattice in packing (Grimes *et al.,* 1998; Lu *et al.,* 1998; Nakagawa *et al.,* 2003; Wu *et al.,* 2000). However, the monomers in all these capsids appear in two configurations, A and B, and assemble as dimers in a *T*=1 pattern.

1.3 POLYMORPH ASSEMBLY

Oligomeric proteins, and other proteins with binding functionality, must be able to discriminate between possible binding targets. The difference in the binding energy of the correct target relative to other potential partners must be sufficiently large. Some proteins are able to assemble into more then one homo-oligomeric structure. Many of these proteins are structural proteins of viruses, which normally assemble into a specifically sized capsid with icosahedral symmetry. Some of these proteins may also assemble an alternative capsid with icosahedral symmetry, but of different size. Proteins that form structures with different symmetries, for instance the VP1 protein of Polyomaviruses, will be discussed later. Why a protein is able to assemble into different structures is obscure. To simplify this complex question on polymorphism the oligomeric protein is sometime discussed as belonging to one or the other of two groups: one where the monomer itself has lost its oligomeric size-discriminating control and one where an additional assembly controller is lacking. The loss of size control is often due to mutations or deletions in the protein. It has been shown many times that deletions in the protein sequence, often N-terminal deletions, can change the shape of the final product (Chen *et al.,* 2000; Sangita *et al.,* 2004; Tang *et al.,* 2006; Hsu *et al.,* 2006). Many proteins seem to have an assembly control where the "correct" protein interactions are induced by association with metal ions, nucleic acids or other proteins (Kellenberger, 1969; Savithri *et al.,* 1983; Salunke *et al.,* 1989; Thuman-Commike *et al.,* 1998; Krol *et al.,* 1999). One intriguing case is the lumazine synthase (LS) from different species, where at least four different types of assemblies appear. A comparison of their crystal structures shows that they have a similar subunit folding, regardless of their assembly states.

1.3.1 Polyomavirus

The structures of both the SV40 and murine polyomavirus have been determined and show a very similar organization where 72 pentamers are arranged with icosahedral symmetry into a *T*=7d surface lattice (Baker *et al.,* 1989; Griffith *et al.,* 1992). The capsids have a diameter of approximately 50 nm. VP1 is the major structural protein and forms the pentameric capsomer of SV40 and murine polyomavirus. These pentamers are built as a ring of five β-barrel shaped VP1 monomers, tightly linked by interacting loops (Liddington *et al.,* 1991; Stehle *et al.,* 1994; Stehle *et al.,* 1996; Yan *et al.,* 1996). The C-terminal domain of each VP1 monomer "invades" a neighboring pentamer, thereby tying the pentamers together in the virion shell. There are six unique monomers in the asymmetric unit forming the capsid (monomers 1-3 at the local 3-fold: orange, blue and green; monomers 4 and 5 around the icosahedral 3-fold: red and cyan and monomer 6 at the icosahedral 2-fold: yellow) (**Figure 1-3a**). The major structural differences between the six unique monomers are found in the C-terminal linking domain and are essential for the formation of the icosahedral capsid (**Figure 1-3b**). The most flexible region in the VP1 protein seems to be the beginning of the N-terminus assumed to be in contact with DNA (amino acids 1-14) and the outermost part of the C-terminal domain (amino acids 355-361). The structure of these regions has not been defined except for the C-terminal part in monomers 2, 5 and 6 (monomer α', β' and γ in Stehle *et al.,* 1996).

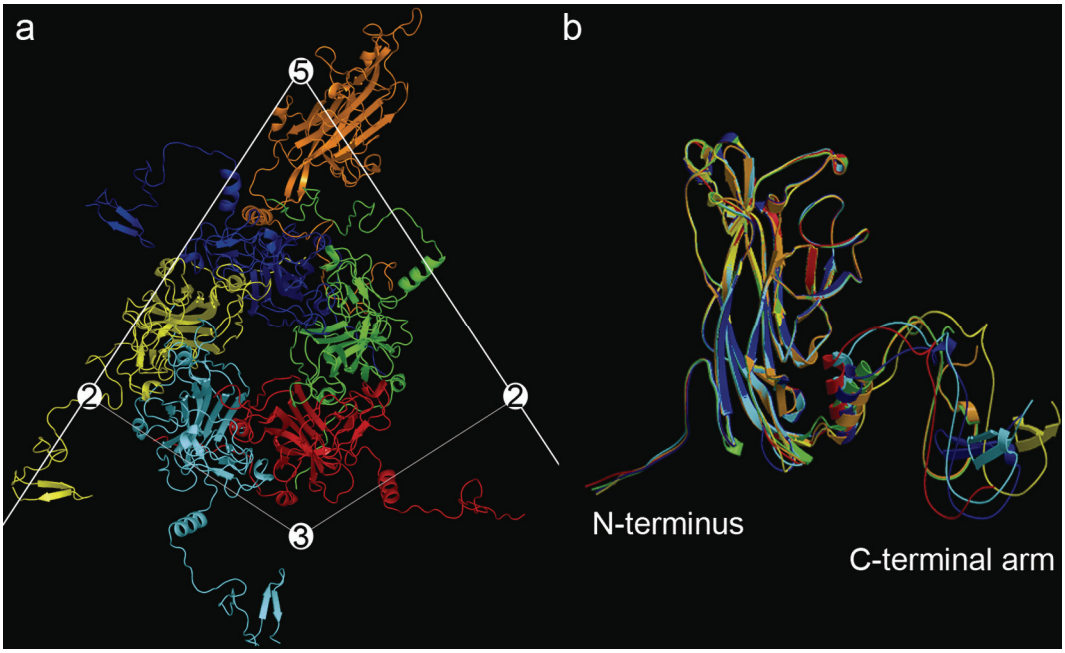

Figure 1-3: The six unique VP1 monomers within the SV40 capsid. (a) Arrangement of the six unique monomers in the asymmetric unit. The symmetry axes are marked with respective numbers as in figure 1-1. (b) The six unique monomers superimposed showing the structural similarities in the core of the VP1 protein and the structural flexibility in the C-terminal arm needed to create a closed capsid.

Both SV40 (Anderer *et al.,* 1967) and murine polyomavirus (Mattern *et al.,* 1967) can assemble into at least four unique particles with different sizes. The particles found after infection of African green monkey kidney cells with SV40 had icosahedral symmetry and a surface lattice corresponding to *T*=1, *T*=3, *T*=4 and the native *T*=7 and diameters of approximately 16.8 nm, 27.4 nm, 31.5 nm and 41.1 nm, respectively. In the case of the murine polyomavirus, infection of mouse embryo cells resulted in three types of icosahedral particles. Their surface lattice and diameters were *T*=1 (22 nm), *T*=3 (38 nm) and *T*=7 (48 nm). Anderer *et al*. (1967) also discovered three different tubular structures with the same diameter as the three particles. The tubular structures were further investigated by Baker *et al.,* (1983) who classified them into two groups in a similar way as was done for the tubular structures of rabbit and human wart papilloma viruses (Finch *et al.,* 1965; Kiselev *et al.,* 1969): "hexamer tubes" for the wide type and "pentamer tubes" for the narrow type. Both types of tubes have a hexagonal arrangement of the pentamers. The wider one has a diameter of 45-50 nm and is found most frequently. However, about 10% of the tubes have a smaller diameter of approximately 30 nm. The two tube structures have two different interpentameric contacts. One is found in both structures and based on edge-to-edge contact. This contact is similar to the interpentameric contact between pentavalent and hexavalent pentamers within the virion. The other contact was identified as the interpentameric contacts between pairs of hexameric pentamers found in the virion. To summarize, all the polymorphic structures of polyomaviruses found so far are built of pentamers. These are connected using one or more of the three unique interpentameric connections found in the native virion. However, the full extent to which these three interpentameric connections can be used in structures with different curvature and size has not been fully explored.

1.3.1.1 Polymorph assembly of polyoma virus-like particles

The VP1 protein of polyomaviruses can be expressed in different cells and can self-assemble into different kinds of structures. It will most commonly assemble into virus-like particles (VLPs), which have the same size, symmetry and surface lattice as the virion (Salunke *et al.,* 1986; Chang *et al.,* 1997; Li *et al.,* 2003) (**Figure 1-4**). These VLPs can, under certain conditions, be disassembled into pentamers and then reassembled. The reassembled particle may have different configurations and sizes depending on the buffer composition. This has been shown for recombinant murine polyoma VLPs (Salunke *et al.,* 1989), recombinant SV40 VLPs (Kanesashi *et al.,* 2003) and recombinant BKV VLPs (Nilsson *et al.,* 2005).

Many studies have demonstrated that calcium ions play an important role in viral assembly (Brady *et al.,* 1977; Salunke *et al.,* 1986; Haynes *et al.,* 1993; Rodgers *et al.,* 1994; Chang *et al.,* 1997; Chen *et al.,* 2001; Ou *et al.,* 2001; Ishizu *et al.,* 2001; Kanesashi *et al.,* 2003; Li *et al.,* 2003; Nilsson *et al.,* 2005). Beside the calcium-binding site, disulfide bonds have also been found to be involved in maintaining capsid stability of the polyomavirus (Walter *et al.,* 1975; Gharakhanian *et al.,* 1995; Chang *et al.,* 1997; Jao *et al.,* 1999; Schmidt *et al.,* 2000; Chen *et al.,* 2001; Ishizu *et al.,* 2001; Li *et al.,*

2002;). Interpentameric disulfide linkages have been identified by X-ray crystallography in the capsid structure of SV40 and murine polyomavirus (Stehle *et al.,* 1994; Stehle *et al.,* 1996).

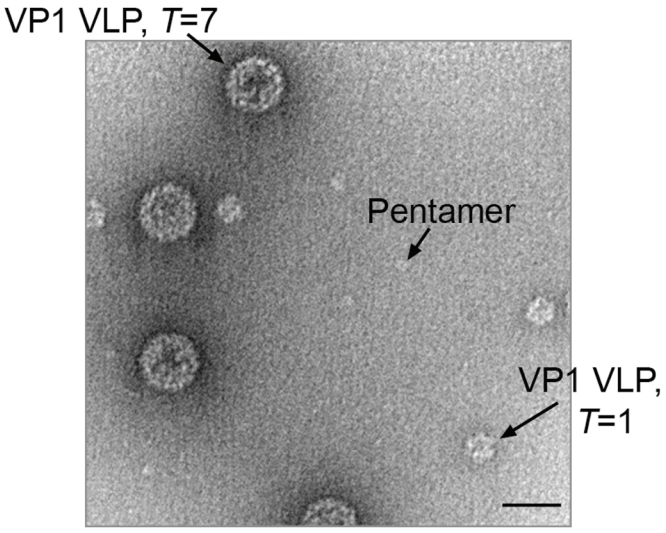

Figure 1-4: Negative stained EM pictures of polymorphic assemblies of BKV VP1 VLPs. The bar corresponds to 50 nm.

1.3.2 Lumazine synthases

The Lumazine synthases have been observed in at least four different types of assemblies: pentamers in *S. cerevisiae*, *M. grisea* and *M. tuberculosis* (Morgunova *et al.,* 2005; Meining *et al.,* 2000; Persson *et al.,* 1999), dimers of pentamers in *Brucella* sp. (Zylberman *et al.,* 2004), *T*=1 icosahedral capsids with an outer diameter of about 160 Å in *B. subtilis*, *Sp. oleraceae* and *A. aeolicus* (Ladenstein *et al.,* 1988; Persson *et al.,* 1999; Zhang *et al.,* 2001) and larger capsids of hitherto unknown molecular structure in *B. subtilis* (Bacher *et al.,* 1986). In *Bacillus subtilis*, the icosahedral capsid of LS encloses a trimer of riboflavin synthase (RS), giving rise to a bifunctional enzyme complex (Bacher *et al.,* 1990). Beside the pentameric and the *T*=1 capsid structures, even larger capsids with an outer diameter of about 290 Å have been observed in pH induced dissociation / association experiments on the icosahedral LS/RS complex from *B. subtilis*. It was found that in 0.1 M Tris/HCl at a pH above 7.0 the complex transforms to larger capsids with a molecular mass of up to 3.6 x 10^6 Da compared to the molecular mass of the native *T*=1 capsid of approximately 1.0 x 10^6 Da (Bacher *et al.,* 1986; Ladenstein *et al.,* 2004). These large particles can be rearranged into hollow *T*=1 capsids by first triggering their dissociation with 6.4 M urea followed by reassembly through dialysis against 0.1 M phosphate buffer, pH = 7.0, containing the substrate analogue, 5-nitroso-6-ribitylamino-2,4(1*H*,3*H*)-pyrimidinedione.

The comparison of crystal structures of the enzymes from different species shows similar subunit folding, regardless of their assembly states. A subunit of lumazine

synthase is formed by a four-stranded β-sheet flanked by two α-helices on one side and three α-helices on the other side. There are however two main parts that differ among the free pentamer form of the monomer and the subunits in the capsid structure. First, the N-termini of the pentameric enzymes are flexible, while in the capsid, the N-termini form an inter-subunit β-sheet with the neighboring monomer within the pentamer (**Figure 1-5a and b**). The second difference is the length of a loop between helices α_4 and α_5 (**Figure 1-5c**). Amino acid sequence alignment indicates that an insertion of 1–4 residues after Gly138 (*S. cerevisiae* numbering) in helix α_4 is unique for the pentameric lumazine synthases. The active sites of LS are located at the interface between two adjacent subunits within a pentameric block. In the icosahedral enzymes, the active sites are close to the inner surface of the hollow capsid as well as close to the pocket at the 2-fold axis (Zhang *et al.,* 2003). Proper assembly of the pentameric block is therefore essential for catalytic activity. The conformation of the active site is highly conserved in all known structures.

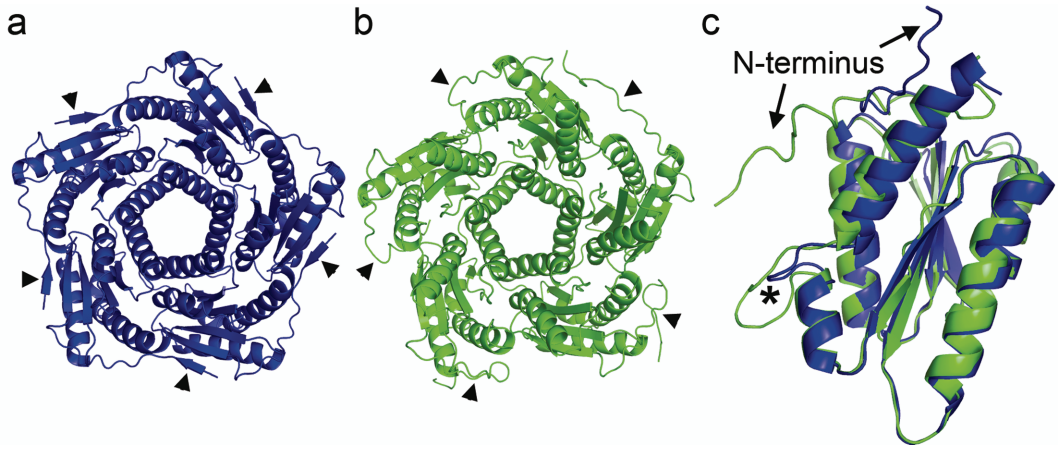

Figure 1-5: Structural similarities and differences between LS that forms *T*=1 capsids and pentamers. (a) The pentamer from the *T*=1 capsid from *A. aeolicus*, and (b) the pentamer from *S. cerevisiae*. The N-termini are marked by triangles. (c) Superimposed monomers from each species showing the two main differences, the N-terminus and the loop between helices α_4 and α_5 (marked with an asterisk) which is four amino acids longer in the enzyme from *S. cerevisiae* (green).

Factors that may affect the assembly of LS have been discussed extensively in earlier studies. It was suggested that Pro8 (*M. grisea* LS numbering) in the N-terminus of the pentameric enzymes hinders the formation of the inter-subunit β-sheet, which is responsible for capsid assembly. It was also proposed that the five residue-kink (GT(G)KAG) found in the C-terminal helix of the icosahedral enzymes plays a role in the formation of the *T*=1 capsid (Braden *et al.,* 2000). A systematic analysis of similarities and differences in pentameric and icosahedral forms of LS designed to identify factors which would determine the quaternary structure was performed by Fornasari *et al.* (2004). Structural comparison and modeling predicts that introducing an insertion of the four amino acids IDEA (Ile, Asp, Glu and Ala) from the *S.*

cerevisiae sequence into the icosahedral LS enzyme from *B. subtilis* would lead to a clash at the interface between pentamers around the 3-fold axis (Meining *et al.,* 2000). This would also be true for the enzyme capsid from *A. aeolicus* (**Figure 1-6**). It was therefore proposed that insertion at this site would inhibit the assembly of *T*=1 icosahedral capsids and thereby promote the formation of free pentamers.

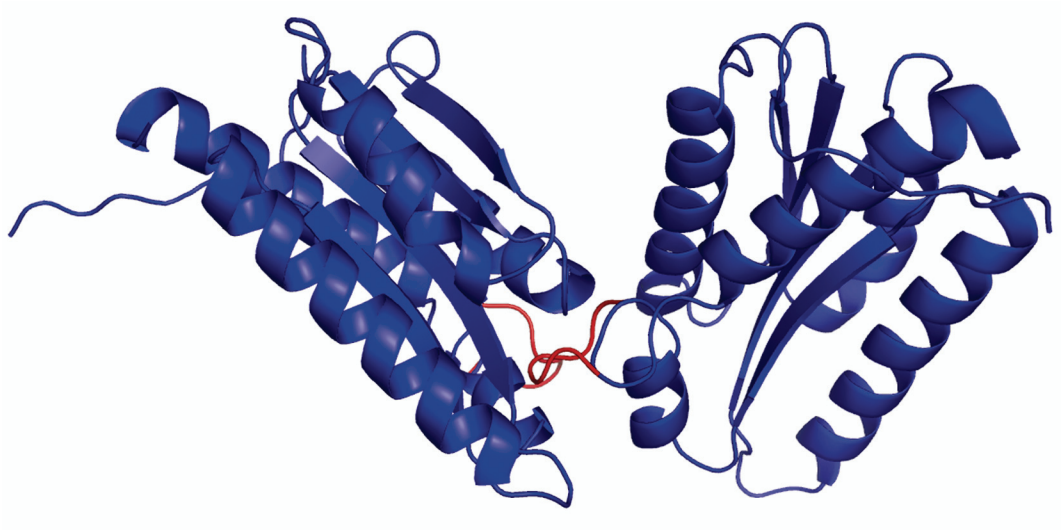

Figure 1-6: Two *A. aeolicus* LS monomers from neighboring pentamers at the 3-fold axis where the IDEA loop has been modeled in (red). In the native *T*=1 structure, the IDEA loop would make a clash at the 3-fold axis with a monomer from the neighboring pentamer.

1.4 POLYOMAVIRUS IN GENERAL AND HUMAN POLYOMAVIRUS BK IN PARTICULAR

Members of the *Polyomaviridae* family are non-enveloped viruses with a circular double-stranded DNA genome of ~5 kbp. The capsid is constructed from three viral capsid proteins (VP1, VP2 and VP3) where VP1 is the major capsid protein, forming the pentameric capsomers of the icosahedral shell. The C-terminal region of the minor capsid proteins VP2 and VP3 is located in the central cavity of the VP1 pentamer (Chen *et al.,* 1998). The rest of either protein have not been structurally determined but should be completely inside the capsid.

The BK virus (BKV) is one of the two known human polyomaviruses. BKV was first discovered in 1971, where it was found in the urine of a renal transplant recipient whose initials were B.K (Gardner *et al.,* 1971). BKV infection is extremely common and occurs in the early childhood. This primary infection with BKV is rarely associated with illness. Almost all illnesses related to BKV occur within the background of immunodeficiency, most often as a result of reactivation of latent virus.

1.4.1 Replication cycle

Productive infection of cells by polyomaviruses can be divided into an early and a late stage. The early stage begins with attachment of the virus to the cell and continues until the beginning of viral DNA replication. After the virion has bound to the receptor

(shown to be N-linked glycoprotein with α(2,3)-linked sialic acid for the BKV (Dugan *et al.,* 2005)), it enters the cell by caveolae-mediated endocytosis (Kasamatsu *et al.,* 1998; Eash *et al.,* 2004). After entering the interior of the cell, the BKV is next transported through the cytosol to the nucleus. This transport is dependent on the active cytoskeletal transport machinery (Dohner *et al.,* 2005). BKV is also assumed to use the microtubule to advance to its intracellular destination (Eash *et al.,* 2005). It is thought that viral DNA enters the nucleus through the nuclear pore complex (NPC) in association with capsid proteins and that uncoating of the polyomaviruses occurs inside the nucleus (Nakanishi *et al.,* 1996; Drachenberg *et al.,* 2003). Once in the nucleus, trancription of an early viral gene (T antigen) is initiated and the mRNA of these genes is transported to the cytoplasm where they are translated. The T-antigens affect the host cell by stimulating the production of enzymes required for cellular DNA replication, thereby preparing the cell for replication of viral DNA. These early viral proteins also stimulate resting cells to re-enter the cell cycle.

The late stage of infection extends from the onset of viral DNA replication to the end of the infection cycle. During this late stage, a transcriptional switch occurs, directing synthesis of the capsid proteins VP1, VP2 and VP3. The VP1 protein, synthesized in the cytoplasm, immediately forms pentamers. These are then associated with VP2 or VP3 and form "heterotypic capsomer complexes". The transport of these complexes into the nucleus is due to the proteins' nuclear localization signals (NLS) (Kasamatsu *et al.,* 1998). In the nucleus, the viral genomes are selected and virion assembly is completed. The newly assembled virions are thought to be released by lytic rupture of the host cell, even though electron microscopy observations report secretion of virions from the plasma membrane of intact cells (Clayson *et al.,* 1989; Imperiale 2001).

1.4.2 Practical use of VP1 virus-like particles

Polyoma VLPs have been found to be useful as transport vehicles for peptides/DNA and as vaccines. They are appropriate immunogen carriers for raising antibodies, not only against the polyomavirus itself, but also against other viruses since it is possible to insert peptides from other proteins into the VP1 loops at the surface of the VLP. Gene transfer into a multitude of different cell types has been extensively tested *in vitro* as well as *in vivo* using VLPs from different polyomaviruses (Forstová *et al.,* 1995; Sandalon *et al.,* 1997; Goldmann *et al.,* 1999; Ou *et al.,* 1999; Kruzewicz *et al.,* 2000; Henke *et al.,* 2000; Yang *et al.,* 2000; Touzé *et al.,* 2001; Clark *et al.,* 2001; Wang *et al.,* 2005). Through modification of the outer loops at the VLP surface, it has been possible to create chimeric VLPs which exhibit cell type specific gene transfer (Gleiter *et al.,* 2001; Stubenrauch *et al.,* 2001; May *et al.,* 2002; Gleiter *et al.,* 2003; Tegerstedt *et al.,* 2005).

It has also been shown that segments as long as 120 amino acids can be inserted into the VP1 protein without disturbing the assembly into VLPs. The immune response against these inserted epitopes has been very high and specific. Thus modified VLPs offer a broad range of potential uses in immune therapy and vaccine development (Gedvilaite *et al.,* 2000; Gedvilaite *et al.,* 2004; Tegerstedt *et al.,* 2005).

Goldmann *et al.* (2000) also show that it is possible to pack small molecules, such as propidium iodide, into the VLPs, suggesting that it would be possible to use polyoma VLPs not only for gene transfer, but also as transporters of pharmaceutical substances.

1.5 GENERAL INFORMATION ON LUMAZINE SYNTHASE

Lumazine synthase catalyzes the penultimate step and the riboflavin synthase the last step in the biosynthesis of riboflavin (vitamin B2). The enzymes LS and RS coexist as a large complex in *Bacillus subtilis*. The complex was first named "heavy riboflavin synthase" and was found to contain two types of functional subunits (Bacher *et al.,* 1980). These were later identified as lumazine synthase (subunit β) and riboflavin synthase (subunit α) (Ladenstein *et al.,* 1986; Bacher, 1986). The crystal structure of the enzyme from *B. subtilis* shows a hollow capsid with icosahedral symmetry and an outer diameter of 15.6 nm. The capsid is built of 60 subunits arranged into 12 pentamers (*T*=1). The overall structure of the native capsid of LS from *Aquifex aeolicus* is very similar to the LS from *B. subtilis* (Zhang *et al.,* 2001). However, it is not know if subunit α is present in the LS from *Aquifex aeolicus*.

1.5.1 Catalytic mechanism

Since humans lack the riboflavin synthesizing enzymes and thus require riboflavin as a vitamin, LS is recognized as a suitable target for antimicrobial therapy. Specific inhibitors of LS are unlikely to interfere with human metabolism. *In vitro* experiments on the wild-type and mutants of LS have revealed considerable insights into the catalytic mechanism of the enzyme (Otto *et al.,* 1981; Lee *et al.,* 1992; Scheuring *et al.,* 2001; Kis *et al.,* 2001; Fischer *et al.,* 2002; Fischer *et al.,* 2003; Haase *et al.,* 2003; Schramek *et al.,* 2003). These results indicate a sequential binding of the two substrates, 5-amino-6-ribitylamino-2,4-(*1H,3H*)pyrimidine-dione and (3S)-3,4-dihydroxy-2-butanone-4-phosphate, to the active site.

The mechanism of how substrates and products are transferred through the capsid wall of the icosahedral enzymes has been investigated in a number of studies (Ludwig *et al.,* 1987; Kis *et al.,* 1995; Persson *et al.,* 1999). The active sites in these structures are located close to the inner surface of the capsid at the interface of two subunits. The channels at the icosahedral 5-fold are the largest openings in the capsid and could serve as the substrate / product diffusion pathway. However, blocking the 5-fold channels of *B. subtilis* LS with the compound $[NaP_5W_{30}O_{110}]^{14}$ did not affect the reaction rate (Ladenstein *et al.,* 1987). Instead, transport of substrates and products, as well as the catalytic state seems to be related to (local) fluctuations in the LS icosahedral capsid. Such dynamic fluctuations could either widen the existing channels or open new ones in the static structure determined by X-ray crystallography.

2 METHODS

2.1 STRUCTURE DETERMINATION

Electron cryomicroscopy (cryo-EM) is the main structural technique used in this thesis. Cryo-EM is an ideal tool to structurally study dynamic events in biological systems. The quick freezing technique can capture biological material (VLPs and enzyme particles in our case) free in solution under nearly native conditions and neither fixation nor staining is required. A density profile of the biological sample can be calculated from EM micrographs using image analysis. The density profile can be fit with the atomic coordinates of each component (protein) separately determined by X-ray crystallography. Molecular interfaces, such as intercapsomeric contacts, can in this way be defined with reasonable precision.

2.1.1 Electron microscopy

2.1.1.1 Preparation of a thin carbon film on 400 mesh copper grids.

Carbon was evaporated onto a freshly cleaved mica sheet in a vacuum chamber using a BIO RAD E6100 control unit. Grids were placed on a filter paper submerged in a water-filled trough. The carbon film was cautiously floated on the water surface above the grids and by lowering the water level, the carbon film was suspended on top of the grids.

2.1.1.2 Negative stain EM.

The 400 mesh copper grids covered with carbon films were made hydrophilic by exposing them to glow discharge using a Baltzers SCD 004 sputter coater. A droplet of the sample (VLPs/enzymes), with a protein concentration of 0.1-0.5 mg/ml, was deposited onto the grid and the excess was blotted off with filter paper. The grids were washed with water before being negatively stained for 15 s using 2 % uranyl acetate.

2.1.1.3 Electron cryomicroscopy (cryo-EM)

Approximately 3 µl of the sample, holding a protein concentration of 1-5 mg/ml, was applied to EM-grids coated with a holey carbon support film. Excess liquid was blotted off with a filter paper and the grid rapidly plunged into liquid ethane, cooled by liquid nitrogen. The rapid freezing rate, greater than 100,000 K/s, prevents ice crystals from forming and preserves the conformation of the protein. A thin (50-100 nm) aqueous film of vitrified ice is produced where the particles are embedded in ice filling the holes in the carbon. After vitrification, the grids were stored in liquid nitrogen until further use. For data collection, the grids were transferred into a Gatan cryo holder and inserted into the microscope while maintaining liquid nitrogen temperatures. The micrographs were recorded using low dose conditions and the same specimen area was exposed twice, first at 1 and then at 3 µm underfocus. Images were recorded using either Kodak SO163 film (Eastman Kodak, Rochester, New York, NY) or a Gatan MegaScan 794/20

CCD camera. Micrographs were collected using either a Philips CM120, a JEOL 300 FEG or a JEOL JEM-3100FFC electron microscope.

2.1.1.4 Image analysis and 3D image reconstruction

Micrographs with sufficiently separated and well-distributed particles, exhibiting minimal astigmatism, were scanned with either a Heidelberg or Zeiss SCAI scanner. Initial particle selection and data processing were done using the RobEM software (http://cryoem.ucsd.edu).

Five parameters were determined for each particle: the θ, φ and ω angles to describe the particle orientation from the cryo-EM imaging, and x and y to describe the center of the particle (*i.e.,* where all the symmetry axes cross). These parameters were thereafter iteratively refined against a successively improved 3D virus/enzyme reconstruction, using the model based polar Fourier transform (PFT) software package (Cheng *et al.,* 1994; Baker *et al.,* 1996). When a stable reconstruction had been achieved, successively higher frequency information was included in further cycles of refinement. Particles to be used in the computation of new refined reconstructions were selected primarily according to their real space cross-correlation coefficients. The computation of the 3D reconstructions included both a high and low pass Fourier filter that suppressed the low and high frequency information. The low-pass filter was set to exclude all frequencies beyond the first zero of the phase contrast transfer function (CTF) so that the reconstruction did not need to be further corrected. Progressively higher spatial frequencies were allowed during the refinement cycles until no further improvements in the structure occurred. The reliability (resolution) of the final 3D reconstruction was determined by Fourier Shell Correlation (FSC) using 0.5 as cutoff. All 3D visualizations were carried out using the IRIS Explorer software (The Numerical Algorithms Group Ltd, Downers Grove USA) that incorporated custom-made modules (L. Bergman and R. H. Cheng, unpublished).

2.1.2 Creation of the BK VP1 model

Structural models of proteins can be created based on the properties of the amino acids along the peptide sequence, and the sequence identity or similarity of domains with those of known structure in other proteins. Information about Cα-Cα distances, secondary structures and residue accessibility aids the success of the model construction. My initial study object was the recombinant BKV VP1 VLP, formed from the major structural protein VP1. The overall primary sequence homology between BKV and SV40 is 69% (Frisque *et al.,* 1984), while the sequence similarity rises to 74% in the VP1 region (Walker *et al.,* 1986). The high similarity between the BKV and SV40 and the SV40 structure solved at 3.1 Å resolution (Liddington *et al.,* 1991) gave us a good template for creating a model of the BKV VP1 protein. The model of the BKV VP1 protein was constructed from SV40 VP1 using the SWISS-MODEL Protein Modeling Server (Schwede *et al.,* 2003) and the software modeler.

2.1.3 Fitting of an atomic model into EM density map

Fitting of the atomic model into the asymmetric unit in the cryo-EM density map was first done manually using O (Jones *et al.,* 1991) for the BKV VP1 VLPs and LSAQ-IDEA. In the final stage of fitting, the positions of the unique monomers were optimized by rigid-body refinement using X-PLOR 3.1 (Brünger *et al.,* 1998). The final model was used to calculate structure factors from which the electron density map was generated at a resolution corresponding to the cryo-EM density (Cheng *et al.,* 1994; Rossmann, 2000). The real-space correlation coefficient between the calculated and the cryo-EM densities was determined using X-PLOR 3.1, CMP or/and the CCP4 suite (CCP4, 1994).

2.2 PROTEIN CHARACTERIZATION

2.2.1 SDS-PAGE

The sodium dodecyl sulfate-polyacrylamide gel electrophoresis (SDS-PAGE) analysis was done using the Phast (GE Healthcare) or mini-Protean® II (Biorad) gel systems according to the manufacturers recommendations. Virus samples were diluted in non-reducing or reducing sample buffer and heated at 95° for a few minutes before added on to the gel (Laemmli 1970). Visualization of the proteins in the gels was regularly done using Coomassie Brilliant blue or silver staining procedures.

2.2.2 MALDI-TOF MS

MALDI-TOF MS: Matrix-Assisted Laser Desorption / Ionisation - Time Of Flight Mass Spectrometry

Mass identity of biomolecules by MALDI-TOF MS was introduced in 1987-1988 by Karas *et al.,* (1988) and Tanaka *et al.,* (1988). The method can be used for detection and characterization of biomolecules, such as proteins, peptides, oligosaccharides and oligonucleotides, with molecular masses between 400 and 350,000 Da.

The sample is mixed with an organic compound that acts as a matrix to facilitate desorption and ionization of compounds in the sample. This mix is then bombarded with laser light which energy will lead to sputtering of the sample and ions from the surface of the mixture. The ionized biomolecules are accelerated in an electric field and enter the flight tube. During the flight in this tube, molecules are separated according to their mass (m) to charge (z) ratio (m/z) and reach the detector at different times (heavier ions are slower than lighter ones). In this way each molecule yields a distinct signal.

2.2.3 N-terminal sequencing

N-terminal analysis of proteins can be done provided that the N-terminal amino acid is not acetylated or otherwise blocked. The proteins to be analyzed have to be pure and should therefore be purified through gel-electrophoresis, I used a SDS 8-25 gradient gel as discussed above, and thereafter transferred to a PVDF membrane. We had to do the sample transfer from the gel to the PVDF membrane through simple diffusion of over night to not loose the small 6kDa band. The PVDF membrane was stained with

Coomassie Brilliant blue and the protein band to be analyzed was cut out. If the bands stain well with Coomassie Brilliant blue there is probably enough protein for N-terminal sequencing.
The N-terminal sequencing was done with Applied Biosystems Procise model 494. This instrument uses Edman chemistry to remove amino acids sequentially from the amino terminus of the protein. The removed amino acids are identified by reverse phase chromatography. Under favorable conditions, the instrument can identify a stretch of fifty amino acids. The sequencing process can not be continued indefinitely since 1 to 10% of the sample may come loose from the supporting PVDF membrane in each cycle. There will also be acid cleavage of peptide bonds. We determined the first 12 amino acids of both the full VP1 protein and the protease cleaved C-terminal arm.

2.3 EQUILIBRIUM DIALYSIS

To study dissociation and reassembly of the VLPs and to see whether the protease cleavage of the VP1 protein had any effect on the particle assembly, home-made dialysis equipment was used that allowed dialysis of small volumes of sample (20-40 µl).

The dialysis equipment:
Dialysis membrane was cut into 1.0-1.5 cm long pieces, which were boiled for 30 s. A dialysis chamber was prepared from a 500 µl Eppendorf tube, using the snap on lid and the top ring of the tube, while the "tube part" was cut away. A hole was punched in the lid and a boiled piece of dialysis membrane clasped between the "tube-ring" and the lid. This small dialysis chamber was placed on a MINI Dialysis Float rack or directly on the surface of the dialysis buffer. The sample to be dialyzed was thereafter added through the hole in the lid. The beaker containing the dialysis buffer and the small dialysis chambers was closed with a plastic lid during dialysis.

3 AIM OF THE THESIS

I have two major goals with this project. First, I want to reveal construction principles and assembly phenomena underlying the dynamic formation of large macromolecular architectures. Along with this, my aim is to extract knowledge that can be utilized for the construction of virus-like particles with defined properties, such as size and stability, surface antigenicity and packing specificity. Thus, in my chosen systems, I am searching for information that is relevant to the design of stable particle-based vaccines, or transport vehicles for DNA, RNA or peptides.

My thesis work focuses on polymorphic systems with intercapsomeric contacts formed by flexible arms or by globular contact surfaces. The first type of contact is studied in recombinant polyomavirus BK particles and the second in the enzyme lumazine synthase. This is approached by the following steps:

- To establish an efficient expression system for the production of BKV VP1 VLPs and to explore the antigenicity and structure of BKV VP1 VLP.
- To explore the polymorphic assembly of BKV VP1 capsids via disassembly / reassembly experiments and structure determination.
- To determine the DNA-VP1 interaction and the role of DNA when it comes to the stability of the BKV VP1 VLPs.
- To define the structure of a large capsid of a lumazine synthase IDEA mutant of *Aquifex aeolicus* and to compare it to the structure of the native enzyme particle.

4 PRESENT STUDIES

4.1 CHARACTERIZATION OF SELF-ASSEMBLED VIRUS-LIKE PARTICLES OF HUMAN POLYOMAVIRUS BK GENERATED BY RECOMBINANT BACULOVIRUSES (PAPER I)

The shell of polyomaviruses has evoked attention due to their unexpected and polymorphic assembly principles. At the time when the quasi-equivalence theory had been settled based on pentameric and hexameric units forming an icosahedral surface lattice in spherical virions, the polyoma system was a true challenge. Not only are all the capsomers pentamers, no hexamers, and still assemble into icosahedral capsids of different size, but they also assemble into helical tubes of different diameters and organizations. This truly polymorphic assembly system (Anderer *et al.,* 1967; Mattern *et al.,* 1967; Salunke *et al.,* 1989; Kanesashi *et al.,* 2003) was selected for study in the present thesis. I am focusing on BK virus, one of the two human polyomaviruses, which are both closely related to the SV40 polyomavirus. Expecting that recombinant BK virus-like particles might retain antigenicity and hemagglutinating activity (HA) similar to the native virus, the study would provides information beyond the theoretical assembly phenomena. Thus, virus-like particles of the BK virus should make it possible to approach both the structural background for polymorphic assembly and to explore assembly principles related to the BK pathogenesis. In addition, suitable carriers for different purposes would be possible to construct. We have set up an expression system with a recombinant baculovirus vector in insect cells (Tn5) that efficiently produces high concentrations of self-assembled BKV VP1 VLP. In this first paper, immunological and structural aspects of the expressed BKV VP1 VLPs are presented.

4.1.1 Results and discussion

The major structural protein VP1 of the human polyomavirus BK (BKV) was expressed using a recombinant baculovirus as vector. The expressed VP1 protein self-assemble into virus-like particles (VLPs) of two different sizes (50 nm and 26 nm in diameter), when expressed in insect cells without the minor proteins VP2 and VP3. Furthermore VLPs with and without DNA were observed. According to the lengths and/or amounts of these incorporated DNA fragments, the BKV VP1 VLPs exhibited different densities. The empty VLPs, which contained no detectable DNA, were 26 or 50 nm diameter and 1.29 or 1.30 g/cm^3 in density. In contrast, the VLPs with a diameter of 50 nm and density of 1.33 and 1.35 g/cm^3 carried cellular DNA of one and three different lengths, respectively.

The VLPs resemble the native BKV virions in their antigenicity and HA activity, therefore the structure of the larger VLPs should have a similar VP1 arrangement as the native virion. The larger VLPs are morphologically indistinguishable from the wild type BK virus when examined by negative-stained electron microscopy. The structure was determined at 20 Å resolution using cryo-EM and three-dimensional reconstruction

and shows similar features to both SV40 and murine polyomavirus (Baker *et al.,* 1988; Griffith *et al.,* 1992) (**Figure 4-1A**). The VP1 is organized into 72 protruding capsomers, which are arranged in a *T*=7d surface lattice. Besides the pentagonal morphology, the density profiles of individual capsomers indicate that all capsomers have only five subunits, which would indicate that the VLPs are composed of 360 subunits. Six unique monomers can be distinguished based on their different local environments (**Figure 4-1B**). These unique monomers give rise to three different intercapsomeric contacts, which can be followed by radially cutting the density of the BKV VP1 VLPs capsid shell reconstruction. One unique interpentameric contact is found at the local 3-fold, connecting three capsomers together. The two other unique interpentameric contacts connected two capsomers, and are found around the 3-fold and at the 2-fold axes.

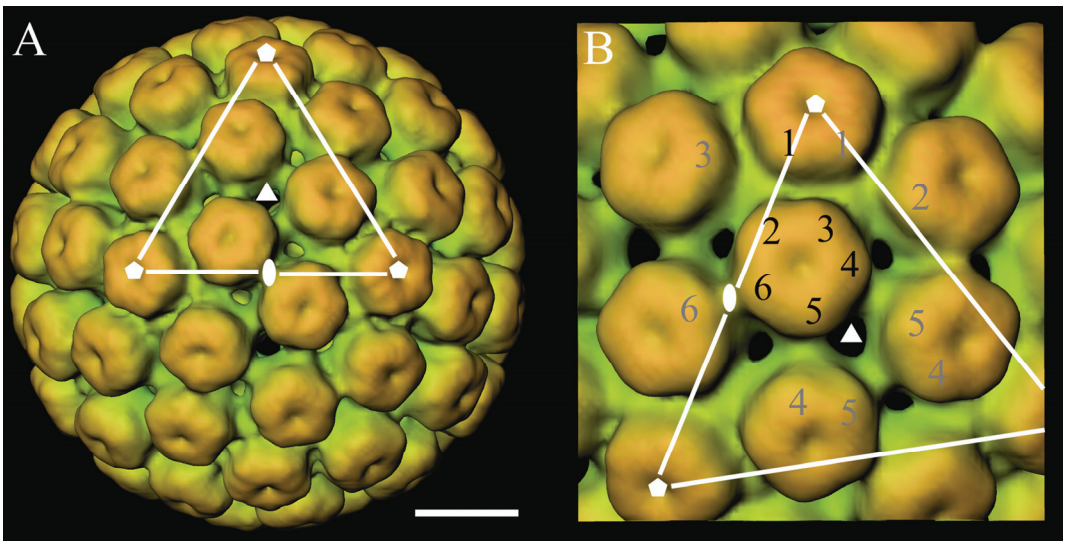

Figure 4-1: Three-dimensional reconstruction of BKV VP1 VLPs. (A) The particle is viewed along the 2-fold axis. The positions of the 2-, 3-, and 5-fold axes are marked with an oval, triangle, and pentagons, respectively. The major capsid protein, VP1, establishes an arrangement according to a T=7d lattice with protruding capsomers at 5-fold and local 6-fold positions. Both capsomers clearly reveal pentameric morphology. The scale bar corresponds to 10 nm. (B) Close-up view of (A) reveals the contacts among the unique subunits. The BKV VP1 VLPs capsid is built up of six unique monomers (marked 1–6). These monomers give rise to three different contacts, represented by subunits 1, 2 and 3 around the pentavalent capsomer, subunits 4 and 5 around the 3-fold axis, and subunit 6 at the 2-fold axis.

Alignment of the primary sequence of BKV VP1 with seven other polyomaviruses, (SV40, Simian agent 12 (SA12), human JC, Budgerigar fledgling disease virus (BFDV), murine polyomaviruses (PyV), Hamster polyomavirus (HaPV) and Lymphotropic papovavirus (LPV)) further indicates that the main differences reside in the top of the pentamer, at the external surface of the capsid shell (**Figure 4-2**). Conserved regions of VP1 among the eight polyomaviruses include the core of the protein and the loops forming the intra and intercapsomeric contacts necessary to form the capsid shell.

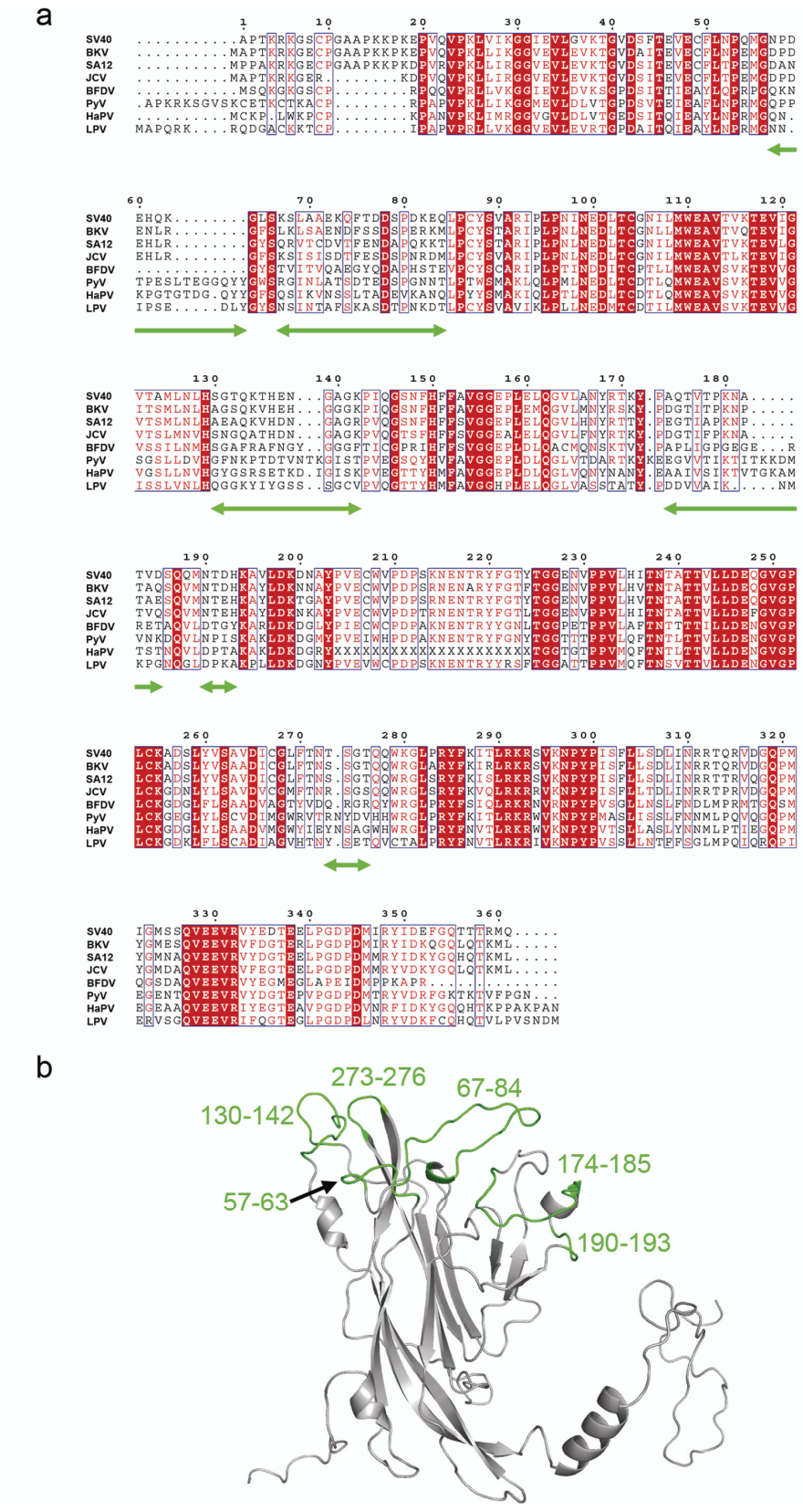

Figure 4-2: Differences and similarities in the primary sequence of the VP1 protein from eight polyomaviruses. (a) Sequence alignment of the VP1 proteins from the eight polyomaviruses SV40, BKV, SA12, JCV, BFDV, PyV, HaPV and LPV. Fully conserved residues are shadowed. The main differences are marked with green arrows and (b) marked as green within the ribbon structure of the SV40 VP1. The alignment was done with the program clustalX and this figure generated using ESPript 2.2.

4.1.2 Conclusions

We have established an expression system that gives high concentrations of BKV VP1 VLPs, which resemble the native BK virions in their antigenicity, hemagglutinating activity and structure. We can now explore the assembly process and specific interpentameric interactions. This will give us insights useful in the handling of problems related to other polyomaviruses, since the main differences of the VP1 among the explored polyomaviruses are found in the outer loops of the VP1, facing the outer surface of the VLP. These differences in the primary structure would account for the unique receptor-binding properties of the different polyomaviruses.

4.2 STRUCTURE AND ASSEMBLY OF A *T*=1 VIRUS-LIKE PARTICLE IN BK POLYOMAVIRUS (PAPER II)

Polyomavirus capsids disassemble into pentamers under certain conditions and can thereafter be reassembled. The reassembled particle may have different configurations and sizes depending on the buffer conditions applied. This was shown for recombinant SV40 VLPs (Kanesashi *et al.,* 2003) and recombinant murine polyoma VLPs (Salunke *et al.,* 1986; Salunke *et al.,* 1989). In the latter case, Salunke *et al.* (1989) showed three types of reassembled particles which differed in size. They concluded from computational modeling that two of the reassembled murine polyomavirus particles had icosahedral symmetry and were composed of 12 and 72 pentamers, in a *T*=1 and *T*=7d surface lattice, respectively. The third type of particle was composed of 24 pentamers with octahedral symmetry. In the present paper, we explore the conditions for disassembly and reassembly of the BKV VP1 VLPs, focusing on conditions that favor one or the other structure. We also examine the structure of the small *T*=1 particle and compare the interpentameric contacts within the *T*=1 and *T*=7d BKV VP1 VLPs (Li *et al.,* 2003).

4.2.1 Results and discussion

The small VLP of BKV VP1 (26.4 nm in diameter) has a *T*=1 surface lattice, with a pentamer located at each 5-fold axis (**Figure 4-3**). In these particles, the main interpentameric contact is found at the icosahedral 3-fold axis. The angle between the pentamers is 38° wider than in the larger BKV VP1 VLP (50.6 nm in diameter). Our observed structure agrees well with the computational modeling of the 12-capsomer murine polyomavirus particle done by Salunke *et al.,* 1989.

Relying on 74 % similarity to SV40 VP1, the primary sequence of BK VP1 was aligned with the coordinates of VP1 from SV40 to create a structural model of the BK VP1 (SV40, PDB:1SVA) (**Figure 4-4**). This model was first fit to the density map of the *T*=7d particle in order to reveal the differences and similarities between SV40 and BKV particles with the same *T*-number. An excellent fit of the VP1 model to the EM-density map was obtained after an adjustment to the slightly larger diameter of the BKV VP1 VLP compared to the SV40 particle. The six unique C-terminal arms, responsible for the interpentameric contacts, fit into the EM density as well.

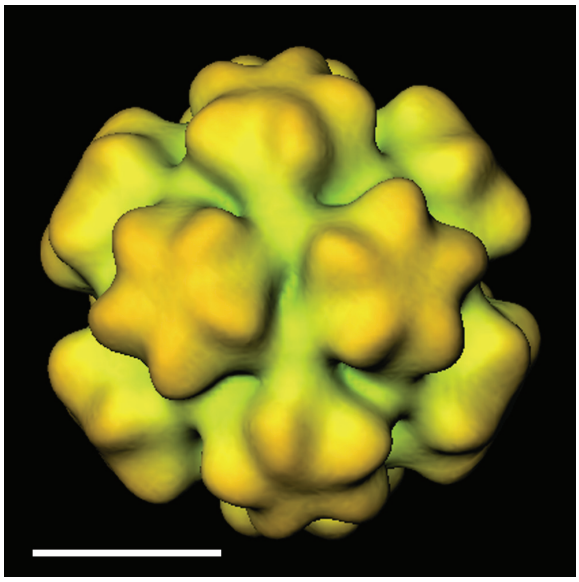

Figure 4-3: Cryo-EM three-dimensional reconstruction of the small BKV VP1 VLP. The particle is viewed along the 2-fold axis. It has icosahedral symmetry, and the VP1 protein is arranged according to a *T*=1 lattice with a protruding capsomer at each 5-fold axes. The scale bar corresponds to 10 nm.

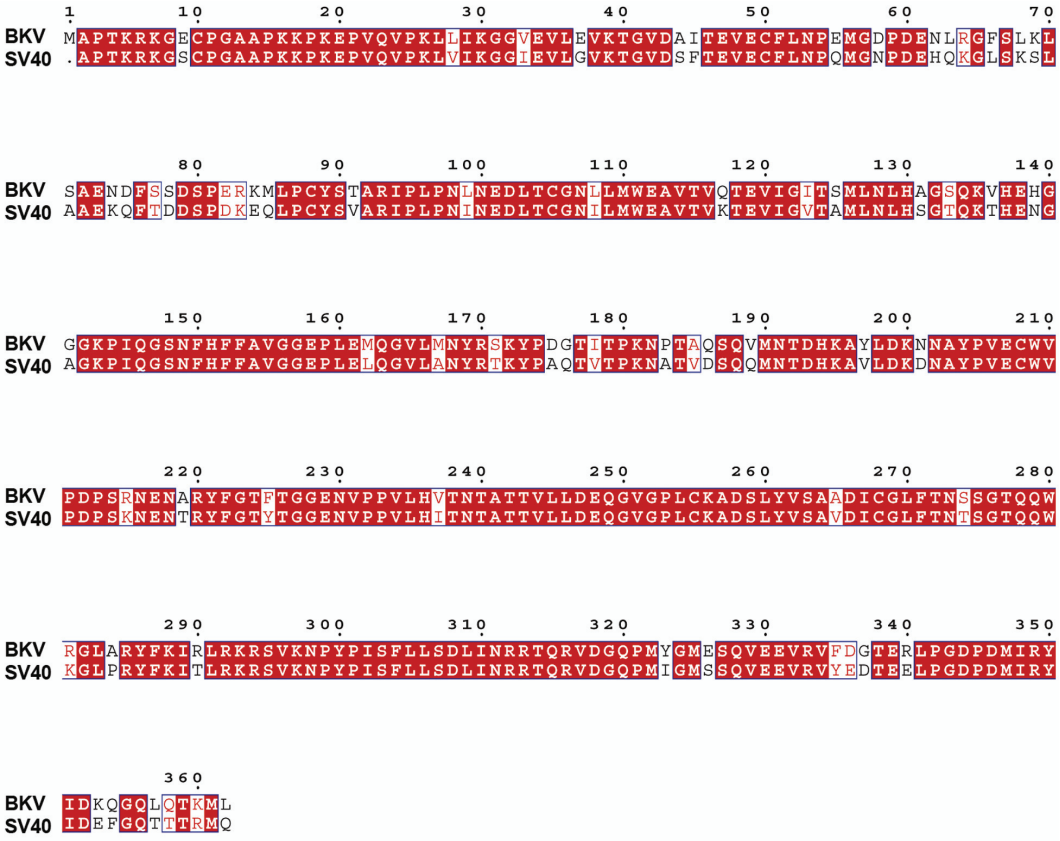

Figure 4-4: Sequence alignment of the VP1 proteins from SV40 and BKV show the possibility of making an atomic model of the BK VP1 from the coordinates of SV40. Fully conserved residues are shadowed. The alignment was done with the program clustalX and this figure generated using ESPript 2.2.

The 5-fold monomer from the *T*=7d BKV structure inserts well into the *T*=1 EM density following an adjustment to the angle between the VP1 core and the C-terminal arm. In *T*=1 particles, the pentamers are connected to each other at the icosahedral 3-fold axes in a similar way as at the local 3-fold axis in the *T*=7d particle. The interaction in both particles appears to be a triple helix bundle (residues 301-313) (**Figure 4-5**). This interaction in the *T*=1 particles appears to have four additional hydrogen bonds and to be less hydrophobic when compared to the *T*=7d structure.
One of the key features of the interacting C-terminal arm, in both the *T*=1 and *T*=7d structures, is the ability of the helix and the following long loop to adjust their position (tilt in different ways) in order to place the J-strand in the correct orientation. The interpentameric interactions involving the J-strand seem to be the most conserved interpentameric contact among the six unique monomers in the *T*=7d structure and the *T*=1 monomer. The outermost part of the C-terminal arm (amino acids 350-362) appear to be the most flexible region, and does not significantly contribute to the stability of either the small or the large VLPs.

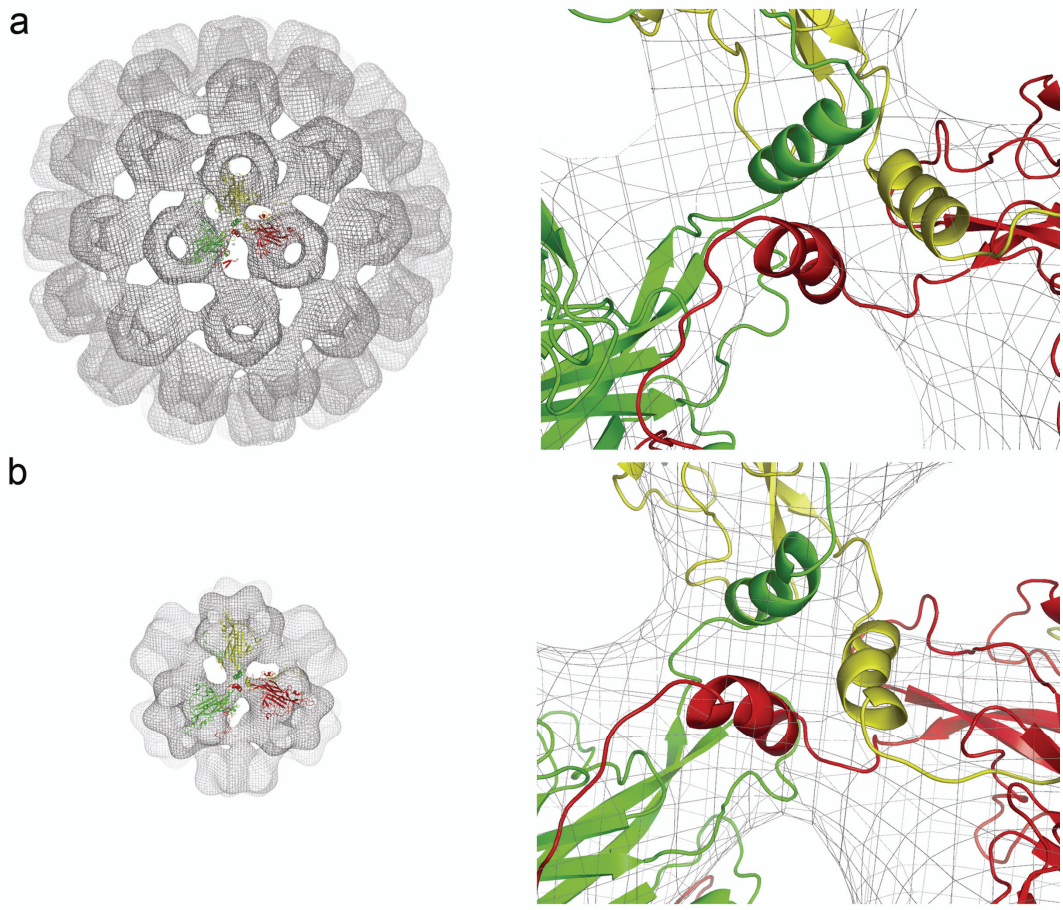

Figure 4-5: Interpentameric interactions in the *T*=7 and *T*=1 BKV VP1 VLP. (a) Left: VP1 model of monomer 1 (yellow), 2 (red), and 3 (green) fit to the density map of the *T*=7d particle at the local 3-fold. Right: close-up of the interpentameric contact "triple-helix bundle" at the local 3-fold. (b) Left: three *T*=1 VP1 models fit to the density map of the *T*=1 particle. Right: close-up of the interpentameric contact found at the 3-fold axis in the *T*=1 particle.

From the results of our dissociation experiments, we conclude that both Ca^{2+} and disulfide links are important for the stability of the *T*=7d capsid. However, at increased ionic strength of the buffer solution, when hydrophobic effects are more influential, the structure kept together also after dissociation of the disulfides. It was thus proven that the hydrophobic effect is essential in keeping the capsid intact. Chen *et al.* (2001) have shown that reducing and chelating agents work in a specific order. The reducing agent has to be introduced in advance to the chelating agent in order for dissociation of the VLPs to occur. Thus, in the disulfide bridged configuration, the Ca^{2+} chelates are not in position to allow the removal of the metal ion. Our reassembly experiments also show that the formation of small or large VLPs do not require the formation of disulfide bonds to assemble *in vitro*. This suggests that the disulfide interaction is not necessary for the actual reassembly process, but that the bond is formed after the particle has been reassembled, allowing for an increase in the stability of the VLP.

Our study has show that small *T*=1 polyoma VLPs can form without calcium, while the larger *T*=7d structure requires calcium ions for assembly. It may be that the interpentameric contacts around the icosahedral 3-fold axis in the *T*=7d particle, in contrast to those at the icosahedral 2-fold or local 3-fold, require calcium for stabilization. The putative calcium-binding amino acids in the C-terminal arm are in position to form salt bridges between adjacent pentamers at the local 3-fold and at the icosahedral 2-fold. This seems not to be possible at the icosahedral 3-fold, since in the absence of calcium ions, the negatively charged amino acids would otherwise repel each other.

4.2.2 Conclusions

In this work, the structure of a small *T*=1 BKV VP1 VLP is solved. We demonstrate that the interpentameric contacts are almost identical despite different configuration in the C-terminal arm of the six unique monomers. The loops before and after the C-terminal helix are the sequence regions that provide the flexibility of the C-terminal arm and allow it to be appropriately positioned. The triple helix bundle contact, found in both the *T*=1 and *T*=7d structure, may represent a common assembly intermediary state, such as one pentamer bound to five other pentamers. In the presence of calcium ions, assembly can continue in a proper way and form the interpentameric contacts around the 3-fold, while without calcium ions, the local 3-fold connections will continue the assembly process into a *T*=1 structure. These ideas agree with the assembly hypotheses of Stehle *et al.,* (1996).

4.3 A 180 SUBUNIT COMPLEX OF A LUMAZINE SYNTHASE MUTANT VIOLATES QUASI-EQUIVALENCE IN CAPSID ASSEMBLY (PAPER III)

It is a general feature of lumazine synthases from different species that they can occur in multiple assembly states. Structural comparison and modeling predicts that introducing an insertion of four amino acids, namely IDEA (Ile, Asp, Glu and Ala) according to the *S. cerevisiae* sequence, into the loop between helices α_4 and α_5, in the icosahedral LS enzyme from *B. subtilis* would lead to a clash at the interface between pentamers around the 3-fold axis (Meining *et al.,* 2000) (**Figure 1-6**). It was therefore proposed that the insertion at this site would inhibit the assembly of a *T*=1 icosahedral capsids and might favor the formation of free pentamers. In the present work, we study the structure of a mutant of *Aquifex aeolicus* LS carrying the IDEA residues inserted subsequent to Gly129, between helices α_4 and α_5. In spite of the insertion the mutated protein assemble into particles. These are larger than the *T*=1 structure. In this paper, we examine the structure of the large mutant particle (LSAQ-IDEA) and compare it to the small *T*=1 LS particle.

4.3.1 Results and discussion

The refined mutant particle structure has a diameter of 292 Å, which is 138 Å larger than that observed in the crystal structure of the native enzyme (**Figure 4-6a**). However, the thickness of the protein shell in the reconstruction (38 Å) is similar to that of the native enzyme. The enzyme complex shows a well-defined 532-symmetry with three unique monomers, referred to as A-C, in the asymmetric unit (**Figure 4-6b**).

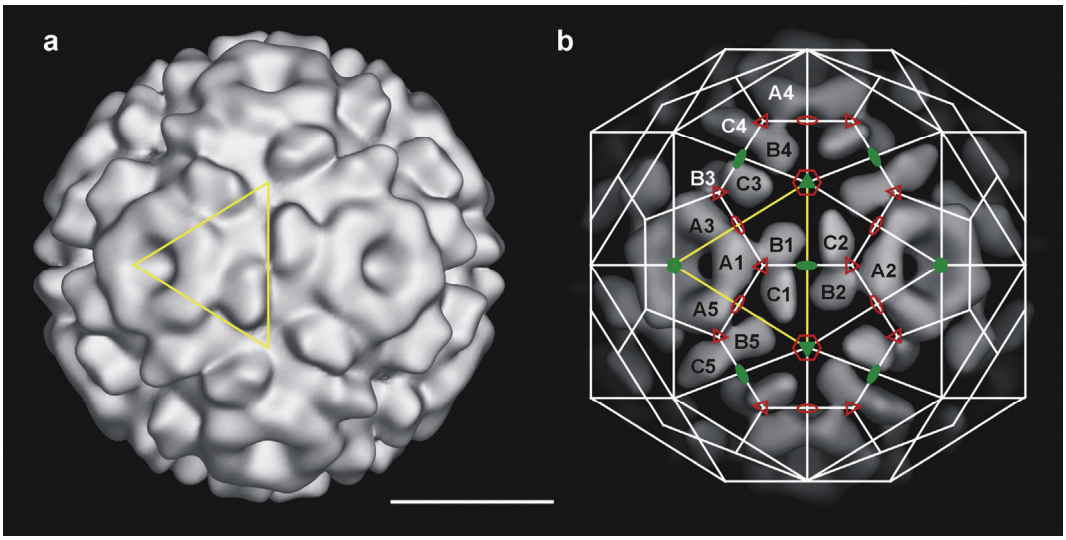

Figure 4-6: The 3D structure of the lumazine synthase IDEA mutant. (a) The LSAQ-IDEA particle is 292 Å in diameter and follows icosahedral symmetry. The bar corresponds to 10 nm. The icosahedral asymmetric unit contains three unique monomers (yellow triangle). (b) The three unique monomers are named A, B and C and numbered in correspondence with the respective asymmetric unit. Filled ovals, triangles and pentagons (green) indicate the location of the strict icosahedral 2-, 3- and 5-fold axes, respectively. Open ovals, triangles and hexagons (red) indicate the locations where the quasi 2-, 3- and 6-fold axes would be expected according to the theory of quasi-equivalence.

The pentamer as well as the channel in the center of the pentamer is approximately 8 Å larger in diameter than the ones found in the smaller *T*=1 particle (**Figure 4-7**). The difference in relative orientation of the pentamer subunits in the *T*=1 capsid and the subunits in the expanded pentamer of the IDEA capsid can be described by a 36º rotation together with a 3 Å translocation away from the 5-fold axis (**Figure 4-8**). This arrangement of the pentamer makes the inserted IDEA-loop point towards the center of the capsid, avoiding the predicted clash.

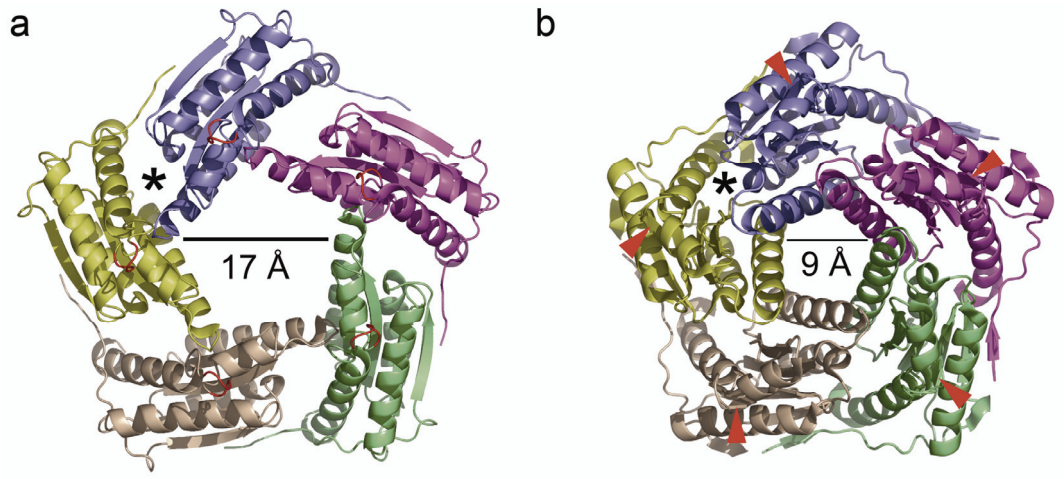

Figure 4-7: Comparison of the pentamers from (a) LSAQ-IDEA and (b) the wild-type *T*=1 LSAQ particle. The inserted IDEA loop is marked in red and the position of Gly129, after which the IDEA motif is inserted in the mutant, are indicated with red arrows. There are five possible active sites in each pentamer, located at the interface of two monomers. One of these interfaces / active sites is marked with an asterisk in each panel. The pentamers are shown from the inside of the capsid.

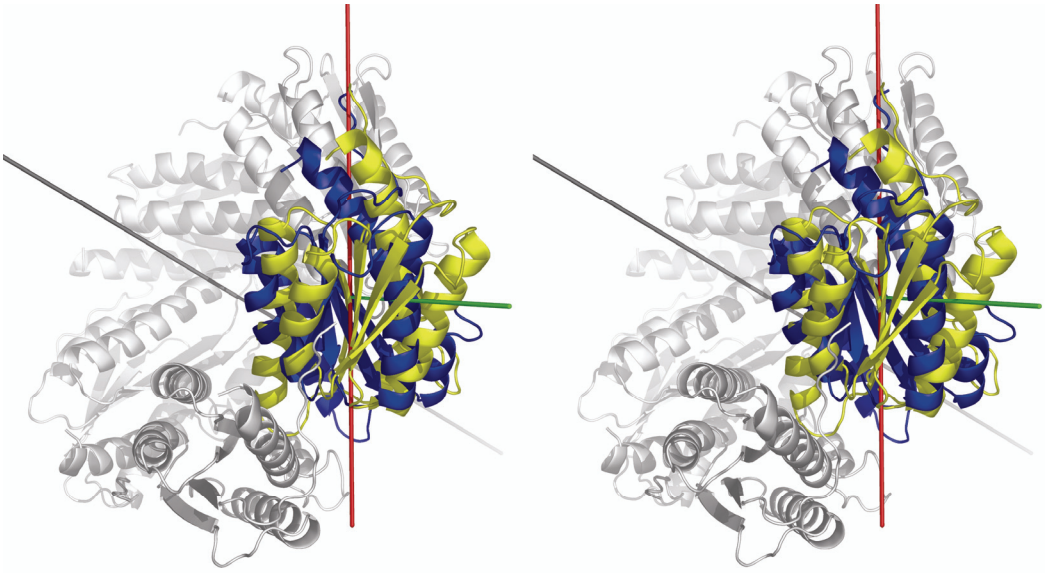

Figure 4-8: The movement needed to transform wild-type LSAQ (*T*=1) subunit from its original location (blue) into the position of the LSAQ-IDEA subunit (yellow). The *T*=1 subunit must move 3 Å (along the green line) out from the 5-fold axis (grey line) and a rotation by 36° (about the red line).

The change in the relative orientation of the subunits within the pentamer results in disruption of the active site, located at the subunit interface (**Figure 4-7**). Consequently, the LSAQ-IDEA capsid is enzymatically inactive (Fischer *et al.,* unpublished result). Some of the important substrate binding amino acids are more exposed in the LSAQ-IDEA pentamer structure than in the wild type. EM studies show that the lumazine synthase from *B. subtilis* can form an enlarged *T*=1 icosahedral particle with an outer diameter of 186 Å (Xing, unpublished results). The pentamers in this enlarged *T*=1 particle are also wider and have a size similar to pentamers from the LSAQ-IDEA particle. This implies that pentamer expansion can happen without destroying the *T*=1 surface lattice and that it may occur as a transition state in the native *T*=1 capsid.

Analysis of subunit interactions shows that the contact surface areas between subunits of LSAQ-IDEA are generally smaller than those of the wild-type enzyme (**Table 4-1**). The average contact surface area, in percent of the total accessible surface area of an isolated monomer, is for a monomer within the LSAQ-IDEA capsid reduced from 49% (wild-type LSAQ) to 20% (LSAQ-IDEA). Compared to contact surfaces of the wild-type enzyme, there are few new contacts observed within the pentamer of the IDEA mutant, *i.e.*, most residues that are involved in the subunit interactions in the pentamer of the mutant are also involved in subunit interactions in the pentamer of the wild-type enzyme. The contacts within the pentamer are mainly formed by hydrophobic residues, both in the LSAQ-IDEA capsid and the wild-type enzyme. Although the contact surfaces between subunits are mainly hydrophobic (64% on average, **Table 4-1**), all contacts involving subunit B and/or C also have a high degree of charged residues. Almost all contacts involving subunit B and C are also new, not seen in the *T*=1 capsid, where the inserted charged amino acids contributes to the interactions within the asymmetric unit. The IDEA loop however does not contribute to the interaction between the pentamer and subunit B. The connecting area of the B subunit to the pentamer is similar to that seen at the 3-fold in the *T*=1 capsid, while the connecting area of the A subunit has changed. Since the jacket surface of the pentamer is changed by a rotation and translocation, the charge-charge connections at the 3-fold in the *T*=1 capsid are exchanged for alternative ones at a more distal location. This accounts for a lower curvature of the growing LSAQ-IDEA particle, which, ultimately results in a smother and larger particle than the *T*=1 LSAQ enzyme.

For a quasi-equivalent surface lattice, interactions located around quasi-m-fold symmetry axes at positions Q_m would be expected to be similar to each other. Furthermore, they would also be similar to the interactions between subunits around related icosahedral symmetry n-fold axes I_n. That means that the intersubunit interactions at Q_2 would be similar to the intersubunit interactions at I_2 and the subunit contacts at Q_6 (which is at the same position as I_3) would be similar to each other and to those at I_5. The contacts between individual subunits within the asymmetric unit at Q_3 would also be similar. However, contact surface comparisons in the LSAQ-IDEA capsid have revealed no similarities between any subunit interfaces at the icosahedral n-

fold symmetry axes and the quasi-m-fold axes. Neither are there any similar contacts between the subunits within the asymmetric unit.

Table 4-1. Surface area calculations of the LSAQ-IDEA mutant and the wild-type LSAQ (Å^2).

		Total ASA (% of [a])	Total CSA [b] (% of [a])	Charged CSA (% of [b])	Polar CSA (% of [b])	Hydrophobic CSA (% of [b])
LSAQ-IDEA	Subunit A (in pentamer)	6721 (79.5)	1734 (20.5)	204 (11.8)	271 (15.6)	1259 (72.6)
	Subunit A (in capsid)	6312 (74.7)	2143 (25.3)	387 (18.1)	283 (13.2)	1473 (68.8)
	Subunit B (in capsid)	6971 (82.5)	1483 (17.5)	325 (21.9)	197 (13.3)	962 (64.8)
	Subunit C (in capsid)	7087 (83.8)	1367 (16.2)	342 (25.0)	279 (20.4)	747 (54.6)
	Averaged (in capsid)	6790 (80.3)	1664 (19.7)	351 (21.1)	253 (16.5)	1061 (63.7)
LSAQ-WT	Subunit in pentamer	5486 (66.2)	2798 (33.8)	408 (14.6)	543 (19.4)	1847 (66.0)
	Subunit in capsid	4231 (51.1)	4053 (48.9)	632 (15.6)	696 (17.2)	2725 (67.2)

[a] Total ASA of an isolated subunit of LSAQ-IDEA and LSAQ-WT are 8454 Å^2 and 8284 Å^2, respectively.
ASA: accessible surface areas
CSA: contact surface areas

4.3.2 Conclusions

The insertion of four amino acids into the loop between helices α_4 and α_5, does not lead to the formation of free pentamers. Instead the mutated protein assembles into an icosahedral capsid with 180 subunits. The subunits are connected in a non-equivalent way, not following the theory of quasi-equivalence.

In the LSAQ-IDEA capsid, the pentamer is widened compared to that of the wild-type enzyme. Such wider pentamers have also been found in enlarged *T*=1 particles (Xing, unpublished results). It would be possible to go from the more narrow pentamer form to the widened pentamer, seen in LSAQ-IDEA, without major steric clashes or destroying the *T*=1 capsid (Zhang, unpublished results), using the rotation and translation motion described above. Thereby, the widened pentamer would allow access to substrate binding or product release and may represent a (hypothetical) intermediate structure in the catalytic cycle.

4.4 THE ESSENTIAL ROLE OF VP1 C-TERMINAL ARM IN POLYOMAVIRUS BK ASSEMBLY AND DNA INCORPORATION (PAPER IV)

The BKV VP1 protein, expressed in insect cells, can assemble into both empty and DNA-containing particles, as shown in paper I (Li et al., 2003). The N-terminal domain of the VP1 protein from different polyomaviruses has been shown biochemically to bind DNA, but no-one has shown structurally how the VP1 protein interacts with DNA in the VLP. We report for the first time the three-dimensional structure of a DNA-containing BKV VP1 VLP, and demonstrate the VP1-DNA interaction site. To do so the structures of empty and DNA-containing BKV VP1 VLPs were determined by cryo-EM and image reconstruction, and our earlier atomic model of the BKV VP1 protein (Nilsson *et al.,* 2005) used to identify the domains involved with DNA binding.

4.4.1 Results and discussion

The structures of empty and DNA-containing VLPs both show 72 pentameric capsomers arranged with icosahedral symmetry according to a *T*=7d surface lattice. Twelve of the pentamers are located at the icosahedral 5-fold axes while the other 60 are positioned at the local 6-fold axes (**Figure 4-9**). The major difference between these two maps is the strong density inside the DNA-containing VLP when compared to the empty VLP. Connecting densities between the VP1 capsid and the inner shell, assigned to DNA, are found near the edge of the local 6-fold pentamers, while no corresponding densities are found connecting to the true 5-fold pentamer.

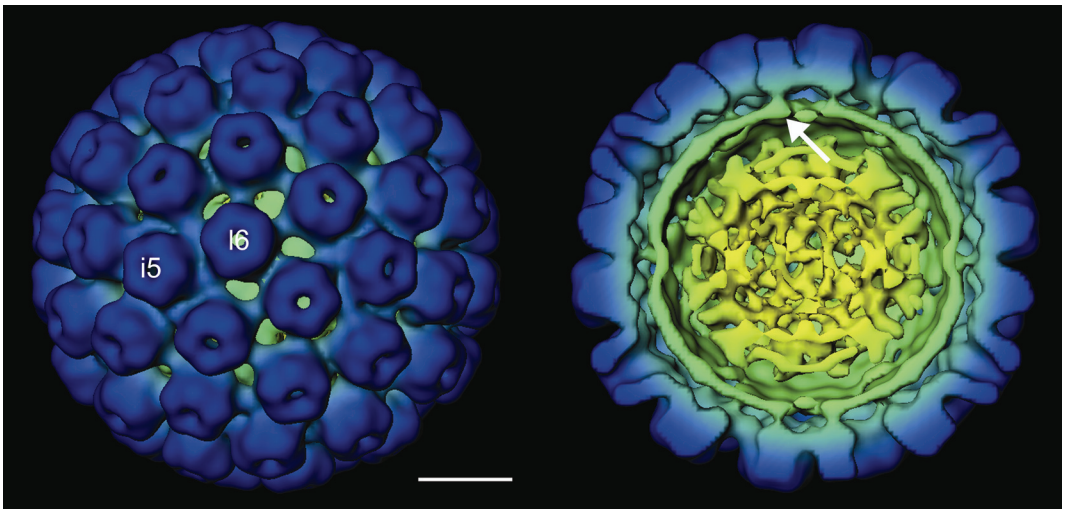

Figure 4-9: Cryo-EM three-dimensional reconstruction of DNA-containing virus-like particles formed by the major structural protein VP1 of BKV. The VLP forms a capsid with icosahedral symmetry where the VP1 protein, in pentameric capsomers, establishes an arrangement according to a *T*=7d surface lattice. The DNA forms an internal shell with contacts to the VP1 capsid (arrow) underneath the local 6-fold pentamers (l6). There are no corresponding densities connecting to the 5-fold pentamer (i5). The scale bar corresponds to 10 nm.

The atomic model of the VP1 protein was fit into the cryo-EM derived structures described above in order to gain a better understanding of the molecular contacts between the capsid and the DNA layer. In our VP1 model, the DNA can interact with amino acids Lys16, Lys17 and Lys19 at the inner surface of the capsid (**Figure 4-10**). The folding of the first part of the N-terminus, which is also assumed to bind DNA, is not known (Stehle *et al.,* 1996). It would, however, be possible for the amino acids 11-15 (Pro-Gly-Ala-Ala-Pro) to form a loop that allows the N-terminus to fold back towards Lys16-Lys19, whereby its Lys5-Arg6-Lys7 motif would come into position for DNA interaction. This structure could be accommodated within the available volume of the DNA connector densities in the cryo-EM structure (**Figure 4-10**).

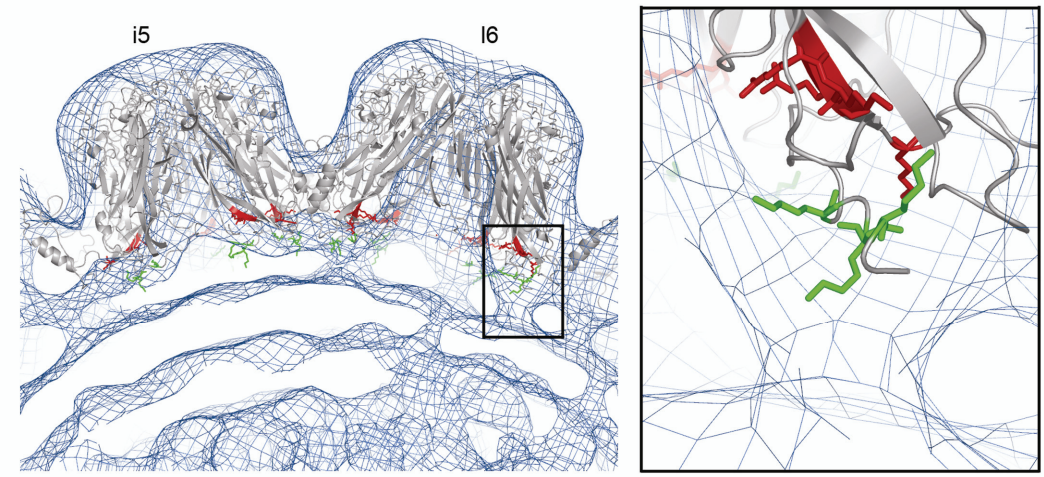

Figure 4-10: Fitting of the VP1 atomic model to the density map of the DNA containing virus-like particle of BKV VP1. Two pentamers are shown from the side, one 5-fold pentamer (i5) and one local 6-fold pentamer (l6). The earlier identified DNA interacting amino acids, Lys16, Lys17 and Lys19, in the N-terminal sequence domain are marked in green and the ones proposed here, Arg292, Lys293, Arg294 and Lys297, in the beginning of the C-terminal arm are marked in red. The boxed area with the DNA contact structure is enlarged in the insert at right.

The beginning of the C-terminal arm (amino acids 281-297) from an adjacent monomer within the same pentamer is located just above the DNA-interacting region of the N-terminus. This subdomain contains seven positively charged amino acids which are all conserved in BKV, JCV, SV40, PyV and SA12 (**Figure 4-2**). In addition an eighth one in the group, Arg290, is present in BKV. At least four of these positively charged amino acids (Arg292, Lys293, Arg294 and Lys297) are in position to interact with the DNA according to our BKV VP1 model (**Figure 4-10**). Single site mutations to alanine were made for each of the eight positively charged amino acids in this group to study their involvement in VLP formation and DNA incorporation.

Mutant VP1 was subjected to density gradient centrifugation to analyze particles that might form. Two of the mutants (Arg281Ala and Arg285Ala) were not able to form VLPs (labelled orange in **Figure 4-11**). These arginines are likely important for the internal stability of the monomer/pentamer and are located high up in the β-sheet, just

before the C-terminal arm. The Lys288Ala, Arg290Ala and Lys293Ala mutants form both empty and DNA-containing VLPs in a ratio similar to the wild-type VLPs (labelled blue in **Figure 4-11**). Three of the mutated VLPs only occur as empty particles (Arg292Ala, Arg294Ala and Lys297Ala, labelled red in **Figure 4-11**). These mutated VLPs have similar density and size as the empty wild-type VLPs and the 260nm/280nm absorbance ratio is also the same (~1.0). No nucleic acids could be found within these three mutated VLPs when analysed by 1% agarose gel electrophoresis. The empty, mutated VLPs look very similar to the empty, wild-type VLPs in negatively stained EM. This indicates that the conserved region (Arg292-Lys297) located just above the DNA interacting N-terminal region is essential for the incorporation of DNA into the VP1 VLP when expressed in Tn5 cells. Their capacity to disassemble-reassemble was compared to see if they also showed behaviour similar to the wild-type particles.

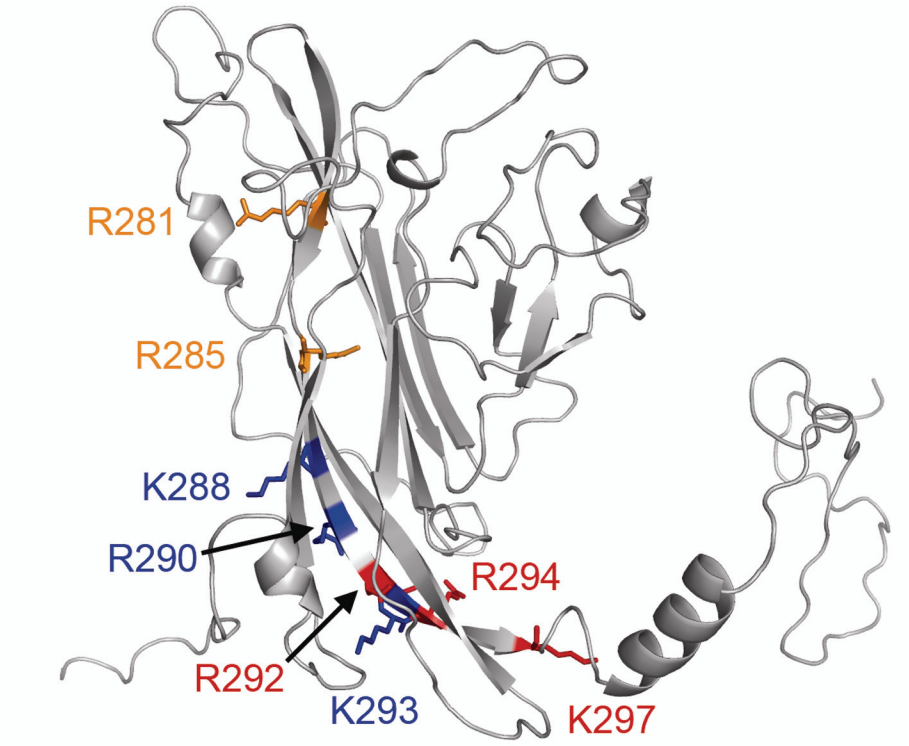

Figure 4-11: Ribbon structure of the BKV VP1 protein model showing the eight single mutation sites.

Empty and DNA-containing wild-type VLPs and empty mutated VLPs could be disassembled into pentamers with EDTA and 2-ME. After disassembly, the free pentamers could be reassembled back into VLPs when dialyzed against a calcium containing buffer (Nilsson *et al.,* 2005). We found that a contaminating cysteine protease cleaves the VP1 protein into peptides of 34 and 6 kDa. This occurrs when the VLPs are disassembled into pentamers. Free pentamers from DNA-containing or mutated VLPs are more resistant towards protease cleavage than pentamers from empty wild-type VLPs, that is, they are only cleaved to about 50%. Through N-terminal

sequencing, the cleavage site was determined to be located between Leu306 and Ser307, in the middle of the C-terminal helix. The protease could not cleave the VP1 protein in the intact VLPs and was inhibited when E-64, Leupeptin or Antipain-dihydrochloride was added to the VLPs before disassembly. The observed cysteine protease activity could originate from V-CATH, a cysteine protease recently found to be encoded by *Autographa californica* M, the parent virus of most common baculovirus expression vectors (Hom *et al.,* 1998). Therefore, care has to be taken to avoid this enzyme to act on the expressed material. In summary, the VP1 pentamers did not reassemble into particles if cleaved, while un-cleaved, disassembled pentamers could reassemble into both *T*=1 and *T*=7 particles. This shows that the C-terminal arm is the most important interpentameric connector and essential for the assembly and stability of both the *T*=1 and *T*=7 structures.

4.4.2 Conclusions

The VP1 shell is structurally similar in both empty and DNA-containing VLPs. A detailed structural investigation of the contact site and additional mutational analyses demonstrate that not only do regions in the N-terminus take part in DNA binding and incorporation, but so also does a positively charged, highly conserved sequence domain at the beginning of the C-terminal arm. Part of this region is essential for particle formation while another is essential for DNA incorporation.

Polyoma VLPs are regarded as highly suitable transport vehicles for drugs, peptides or DNA, and as carriers of vaccine antigens inserted into the VP1 loops at the surface of the particles. The three empty single site mutant VLPs presented here might perform this task better than the wild-type VLP, eliminating risks associated with contaminating DNA.

5 GENERAL DISCUSSION

In this study, I have focused on the icosahedral framework in virus-like particles from the human polyomavirus BK and the enzyme lumazine synthase from *Aquifex aeolicus*. This was done by exploring how a single type of building unit can assemble into particles with different size and surface morphology. The two systems are different in that the BKV VP1 protein forms pentamers which interact through long (approximately 60 amino acids) flexible arms, while the enzyme protein is more globular, forms pentamers without protruding domains and therefore interacts using globular surfaces. In both cases hydrophobic effects seem to be the main stabilizing force when it comes to the formation of the capsomers (pentamers), while the assembly of pentamers (or connection of subunits to the pentamers) in addition require more specific interactions.

Flexibility and assembly

In the BKV VLP the main flexibility is found within the C-terminal arm, which forms the main interpentameric contact and it is there that we find the assembly control exercised by a calcium ion. In the lumazine synthase case the active site is located at the subunit interface within the pentamer, where the prosthetic group would control the needed motion for binding substrates and releasing products. Therefore, both systems requires an external assembly control; calcium ions in the case of BKV VLPs and phosphate and/or substrate for the *T*=1 capsid of lumazine synthase. No structures of lumazine synthase has been solved without at least the phosphate bound to it, in most cases a substrate-analog or inhibitor has been present too.

The dynamic contact

The general hypothesis is that icosahedral particles obtain their dynamic properties from flexibility of the structure in the subunit contact domains, while the structure of the core of the subunits remains stable. This seems to be true for both the VLPs and enzyme-like particles even though their defined sources of flexibility are different. As mentioned above, the VLPs primarily use the two loops, before and after the C-terminal helix, to adjust the position of the flexible arm so that the intercapsomer interactions can be kept as similar as possible even at different symmetrical environments and particle curvatures. This type of quasi-equivalent contacts could not be found between subunits at non-symmetry related environments in the LSAQ-IDEA particle. Therefore, the flexibility is not the result of different folding of a connector arm. Instead different areas of the protein surface can form the interaction. Here, hydrophobic areas together with patterns of complementary charges are involved. One can think of the interpentameric connections in the enzyme as hooks and loops in a Velcro fastener where the interacting areas can be utilized and combined in different ways, use half or all of it, or rotate it. In all cases, one will still have a more or less stable attachment.

The theory of quasi-equivalence

Structural variability and adaptability in intercapsomeric contact domains is necessary, for instance during the particle formation, and remains often as a quasi-equivalent pattern within the icosahedral capsid. This phenomenon is explained by the quasi-equivalence theory, as discussed in the introduction. As with most rules or theories, there are exceptions or at least observations that stretch the boundaries that initially led to the rule or theory. In this thesis, we have dealt with two such systems. The BKV VLP system stretches the boundaries that were set up for the quasi-equivalence theory. Whereas the LSAQ-IDEA particle is to be regarded as an exception in the sense that alternative contacts are taken in the alternative configurations. This type of flexibility in an icosahedral structure might be possible where the surface provides alternative contact domains. Although the type of interaction would be the same, the residues involved are not the same in the particles of different size. The LSAQ-IDEA case violates not only the original concept of quasi-equivalence, suggesting that the same interaction is flexible enough to allow contact between subunits at non-symmetry related environments, but also represents a solution to another need of a new dynamic arrangement.

Transitions between states

With the similar size and properties as LSAQ, the icosahedral lumazine synthase capsid from *Bacillus subtilis* can be disassembled by increasing the pH and decreasing the phosphate concentration. The units can be reassembled into large particles with the same diameter as our LSAQ-IDEA particle. Furthermore, these particles if disassembled and again reassembled in the presence of substrate-analogous ligands, formed native sized particles (Bacher *et al.,* 1986). These "*native"* large particles may differ in their interpentameric contacts from those in the LSAQ-IDEA, due to the insertion, which could influence the configuration. However, the wide pentamer configuration we see in LSAQ-IDEA does not include interactions directly with the insertion. The transition from the narrow pentamer of the *T*=1 capsid to the wider pentamer seen in the LSAQ-IDEA capsid mainly involves a 36 degree rotation away form the 5-fold axis (for more details, see paper III). This could well be a transition happening within the *T*=1 native particle on release of cofactor or substrate. It is anticipated that this occurs in the slightly larger *T*=1 LS capsid from *B. subtilis* (Xing, unpublished results). Therefore it would be possible to go from one capsomer configuration to another. This could reflect a catalytic transition naturally occurring in lumazine synthase particles.

Bioengineering aspects

While observing the variations occurring in the different assembly situations studied, my aim has been to extract knowledge that can be utilized for the construction of virus-like particles with defined properties, like size and stability, surface antigenicity and packing specificity. Two types of assembly mechanisms have been identified. Both are using a stable self-assembling pentamer as building blocks. While the polyoma virus

model elaborates on capsomers linked together by flexible arms, the lumazine synthase system, as we have shown, provides surfaces with alternative contact domains. Both systems can be adopted for various purposes. The polyoma particles, as shown, can be designed to encapsulate nucleic acid, and thus be used for gene delivery, or constructed to avoid nucleic acid incorporation. The exterior loops are not involved in assembly and would provide attachment sites for antigens or receptors to target particular tissues or cells. The same holds for the lumazine synthase particles, which can be made flexible for cargo uptake and delivery or as a rigid inactive structure for small strategically placed insertions, preventing flexibility, but retaining the self assembly property. The control of assembly has been extensively explored. In my chosen applications, I have been searching information that is relevant for the design of stable particle-based vaccines, or transport vehicles for DNA, RNA or peptides. Although the results are modest in the wide field of such applications, my hope is that the findings here described will find their use and be beneficial for further applications.

6 FUTURE PERSPECTIVES

Big things have small beginnings. This holds in particular for the assembly of giant molecules like virus shells and similar constructs. The fact that multiple copes of a single molecule can form a stable spherical shell is fascinating in itself. It becomes even more so when considering that one and the same building unit can be used in constructions of different size and sometimes different shapes. The two polymorphic systems studied in this thesis provide examples on this phenomenon. The results presented, combined with knowledge gained from studies by others, show that it is possible to control the assembly pathway and thereby the end product. Simple physical principles, like ion strength, pH, reducing potential and the concentration of a particular component can be used to guide the assembly pathway into different end-products with high fidelity. Proteins that naturally self-assemble into capsids seem to be well adapted to this function and usually allow ample of opportunities to modulate other domains. As found here, the building unit uses defined domains for the association, although these might be slightly different in different architectures. This leaves domains available for modulation to introduce new functions. There is indeed a window for opportunities to engineer the capsid surface to better selectivity in cell recognition, or to equip the capsid interior to better encapsulate the target of choice. While viruses by tradition have been the main focus in particle biotechnology, there is nowadays a growing interest for other biological particles, like the Lumazine synthase (Sciutto *et al.,* 2005; Seebeck *et al.,* 2006). The viruses naturally provide a cell targeting structure; the selected giant enzyme would provide alternatives to be explored. The approach taken in this thesis has been to explore the assembly principles by a careful structural analysis. This provides the information necessary to engineer novel delivery containers and vaccine particles. My wishes for further development in these areas are to find means for targeted drug delivery, which would minimize toxic and other side effect, but still maintain an efficient targeting control.

7 ACKNOWLEDGEMENTS

Many people have helped me in different ways during my time as a Ph.D. student, in the process of research, with writing and last, but not least, encouraged me when needed. I would therefore like to give my sincerely thanks to the following people.

Thanks to my supervisors:
Professor Holland Cheng, for giving me the opportunity to carry out my Ph.D. in your lab and for letting me develop into an independent person. Thank you for putting me in the driving seat of my project from the early beginning, which forced me to learn how to set up a project and how to finish it.

Associate Professor Lena Hammar, thank you for all help during these years, from the start of my exam work to the finish-line of my Ph.D. thesis. You have always been there for project discussions as well as for more personal discussions. The group had not survived without you!

Professor Anders Vahlne, thank you for taking time from a very busy schedule and for giving me the feeling that I could always turn to you if needed. I would also like to thank you and Tripep AB for the great financial support as a truly committed sponsor during these years.

I'm thankful to the board of the Ph.D. Program in Biotechnology with an Industrial Focus for letting me attend the program. Thank you Agneta Mode for all support as well as for very interesting and well organized courses. I would also like to thank Pia Hartzell for always being there when I needed help with my budget.

Thanks to all my present and former colleagues in the HCH-group:
Lars Haag, för att du är en sådan god vän och kollega. Hade aldrig klarat mig igenom detta om du inte hade funnits i gruppen. Att få arbeta med någon som man uppskattar så mycket är få förunnat men det har gjort saker och ting mycket lättare.

Sunny Wu, for that you always stands up for what you believe in and never do things that you think are wrong. You are such a lovely person, even when times are more than rough.

Joseph Wang, you are one of the most kind and caring person that I have ever met. You are also very skilled in what you are doing and I wish you all the best in the future.

Dr. David Morgan, for all time you spent critically reading my manuscripts and thesis, I think and hope that you know what that have meant to me. I also want to thank you for interesting discussions during the morning coffee-breaks out in the sunshine in Davis.

Saharat Aungsumart, what can I say, you are such a terrific student and the BK-DNA project would not have been done in such a good way without you. I wish you all the best in the future!

Dr. Li Xing, for letting me join the lumazine project, I have learned a lot from our project discussions and how to perform pdb-rearrangements. I have also very much enjoined your company during all conferences that we have attended. Best wishes for you and Xiao!

Leif Bergman, what should I have done if I didn't have you to bicker with every day! You ones said the nicest thing to me "…that I haven't become the computer nerd that I should have been after so many years here". Love you for that, which also means that I really have to thank you for all help with computer problems!

Dr. Bomu Wu, for teaching me how to use our reconstruction programs, to understand icosahedral symmetry, T-numbers and for all interesting discussions about China.

Dr. Naoyuki Miyazaki, for good collaboration and for teaching me about modeling.

I would also like to thank all former group members, not mentioned above, that I have had the opportunity to work with. Anders, Nicklas, Ruchi, Igor, Wit, Fredrik, Helena E, Helena S and Willhem thank you all for a very nice time.

Thanks to all my collaborators for your work and our discussions, which have been essential for my personal development and this thesis:
Professor Tatsuo Miyamura, you are a person that I deeply admire both as a scientist and as person. Thank you so much for letting my stay in your lab, for all great scientific discussions and for creating such a nice working environment.

Dr. Naokazu Takeda, for all the help during my stay in Tokyo, for example the arrangements that made it possible for me to use your EM in Murayama.

Dr. Tian-Cheng Li, for all fantastic work that you have done for my projects. You have always made me feel so welcomed in your lab and helped me during my stays in Tokyo. I really hope that we will be able to stay in touch.

Dr. Kenzo Kato, for very interesting discussions about the BK virus and for excellent sightseeing in and outside Tokyo.

Professor Rudolf Ladenstein, Dr. Winfried Meining and Dr. Xiaofeng Zhang, Professor Adelbert Bacher, Dr. Ilka Haase and Dr. Markus Fischer for a very encouraging collaboration, I learned a lot from you guys.

To all colleagues in the HGA-group: Henrik Garoff, Birgitta Lindqvist, Rickard Nordström, Maria Hammarstedt, Mathilda Sjöberg, Robin Löving, Shujing Zhang, Helena Andersson, Michael Wallin, Maria Ekström, Malin Kronqvist and Kejun Li whose help and company I have appreciate very much.

I would also like to thank Kristina Bergholm for helping me with all administrative questions.

And a big thank you must go the Cecilia Tilly, Åsa Björck, Jessica Odefjärd and Linda Sundell for helping me with my budget and letting me go through your folders for missing invoices.

Lars Uppvall, för att du alltid finns där för mig. Utan dig hade jag absolut inte klarat den här tiden. För att du funnits där och pushat mig då jag inte orkat mer men även sagt till mig då det varit dags att ta en dag ledigt. Tror och hoppas att du vet hur pass delaktig du är i det här arbetet men framför allt i mitt liv. Älskar dig!!

Mamma och Pappa, Ann-Louise och Jörgen Nilsson, vet inte riktigt vart jag ska börja, och sluta är i princip omöjligt. Tack i alla fall för att ni alltid finns där och för att ni har lärt mig att tro på mig själv, något som verkligen har behövts både en och två gånger. Älskar er!!!

Katarina Nilsson, jag är så stolt över att få vara din syster och snart även en mycket stolt moster. Hoppas att du åtminstone till en del anar hur mycket du betyder för mig och att veta att du alltid finns där betyder allt.

Christian Sehler, tack för att du är en underbar man till min syster. Du ska veta att just detta är inget som jag tar lätt på, men du gör mitt liv så mycket enklare då jag vet att hon alltid har dig.

Farmor, Vivi Nilsson, har nog dig att tacka för det mesta i den här avhandlingen, hade jag inte ärv åtminstone delar av din envishet så hade jag aldrig stått här idag.

Anna-Lisa Mattsson, för att du har visat mig att man kan mycket mer än man tror bara man bestämmer sig för det.

Gunbritt Uppvall och Jan Uppvall, ja det är väl ganska självklart, tack för den bästa pojkvännen i hela världen!!!!

Åsa Forslöf, Agneta Torstensson, Sara Strandberg och Linn Karlsson för att ni är de bästa vänner man kan ha, för att ni fortfarande ringer mig trots att jag så många gånger har sagt att jag måste jobba, har inte tid. Har haft så fantastiskt många roliga stunder med er och hoppas på ännu fler så småningom.

Mami Matsuda, for taking so good care of me in Tokyo, it has been so nice to getting to know you. I hope that I will travel to Tokyo some more times and that we can meet there again.

Mohamed Homman, for coming by now and then, which always lighten up our daily life.

This work was supported by Tripep AB and the Foundation for Knowledge and Competence Development, The European Community Sixth Framework Programme LEVMAC, and the Karolinska Institute.

8 REFERENCES

Anderer, F. A., Schlumberger, H. D., Koch, M. A., Frank, H. and Eggers, H. J. (1967). Structure of simian virus 40: II. Symmetry and components of the virus particle. *Virology*, 32:511-523.

Bacher, A., Baur, R., Eggers, U., Harders, H. D., Otto, M. K. and Schnepple, H. (1980). Riboflavin synthase of *Bacillus subtilis*. Purification and properties. *J. Biol. Chem.,* 255:632-637.

Bacher, A. (1986). Heavy Riboflavin synthases from *Bacillus subtilis. Methods in Enzymology,* 122:192-199.

Bacher A and Ladenstein R. (1990) The Lumazine Synthase/Riboflavin Synthase Complex of Bacillus subtilis. In *Chemistry and Biochemistry of Flavoenzymes*, Müller F (ed), I. pp 215-259. Boca Raton, Florida.: Chemical Rubber & Co.

Bacher, A., Ludwig, H. C., Schnepple, H. and Ben-Shaul, Y. (1986). Heavy Riboflavin synthases from *Bacillus subtilis*, Quaternary structure and reaggregation. *J. Biol. Chem.,* 187:75-86.

Baker, T. S., Caspar, D. L. D. and Murakami, W. T. (1983). Polyoma virus 'hexamer' tubes consist of paired pentamers. *Nature*, 303:446-448.

Baker TS and Cheng RH. (1996) A model-based approach for determining orientations of biological macromolecules imaged by cryoelectron microscopy. *J Struct. Biol.,* 116:120-130.

Baker, T. S., Drak, J. and Bina, M. (1988). Reconstruction of the three-dimensional structure of simian virus 40 and visualization of the chromatin core. *Proc. Natl. Acad. Sci. USA,* 85:422-426.

Baker, T. S., Drak, J. and Bina M. (1989). The capsid of small papova viruses contains 72 pentameric capsomers: direct evidence from Cryo-EM of simian viurs 40. *Biophus J.,* 55(2):243-53.

Braden, B. C., Velikovsky, C. A., Cauerhff, A. A., Polikarpov, I. and Goldbaum, F. A. (2000). Divergence in macromolecular assembly: X-ray crystallographic structure analysis of Lumazine synthases from *Brucella abortus*. *J. Mol. Biol.,* 297:1031-1036.

Brady, J. N., Winston, V. D. and Consigli, R. A. (1977). Dissociation of polyomavirus by the chelation of calcium ions found associated with purified virions. *J. Virol.,* 23(3):717-24.

Brenner, S. and Horne, R. W. (1959). A negative staining method for high resolution electron microscopy of viruses. *Biochim. Biophys. Acta,* 34:103-110.

Brünger AT, Adams PD, Clore GM, DeLano WL, Gros P, Grosse-Kunstleve RW, Jiang JS, Kuszewski J, Nilges M, Pannu NS, Read RJ, Rice LM, Simonson T and Warren GL. (1998) Crystallography & NMR system: A new software suite for macromolecular structure determination. *Acta Crystallogr D,* 54**:**905-921.

Caspar, D. L. D. and Klug, A. (1962). Physical principles in the construction of regular viruses. *Cold Spring Harbor Symp. Quant. Biol.,* 27:1-24.

Chang, D., Fung, C. Y., Ou, W. C., Chao, P. C., Li, S. Y., Wang, M., Huang, Y. L., Tzeng, T. Y., and Tsai, R. T. (1997). Self-assembly of the JC virus major capsid protein, VP1, expressed in insect cells. *J. Gen. Virol.,* 78:1435-1439.

Chen, PL., Wang, M., Ou, WC., Lii, CK., Chen, LS. and Chang, D. (2001). Disulfide bonds stabilize JC virus capsid-like structure by protecting calcium ions from chelation. *FEBS letters.* 500:109-113.

Chen, X. S., Stehle, T. and Harrison, S. C. (1998). Interaction of polyomavirus internal protein VP2 with the major capsid protein VP1 and implications for participation of VP2 in viral entry. *EMBO J.*, 17(12):3233-3240.

Chen, X. S., Garcea, R. L., Goldberg, I., Casini, G. and Harrison, S. C. (2000). Structure of small virus-like particles assembled from the protein of human papillomavirus 16. *Molecular cell,* 5:557-567.

Cheng RH, Reddy VS, Olson NH, Fisher AJ, Baker TS and Johnson JE. (1994). Functional implications of quasi-equivalence in a T = 3 icosahedral animal virus established by cryo-electron microscopy and X-ray crystallography. *Structure* 2:271-282.

Clark, B., Caparrós-Wanderley, W., Musselwhite, G., Kotecha, M. and Griffin, B. E. (2001). Immunity against both polyomavirus VP1 and a transgene product induced following intranasal delivery of VP1 pseudocapsid-DNA complexes. *J. Gen. Virol.,* 82:2791-2797.

Clayson E. T., Brando L. V. and Compans R. W. (1989). Release of simian virus 40 from epithelial cells is polarized and occurs without lysis. *J. Virol.* 63:2278–2288.

Crane, H. R. (1950). Principles and problems of biological growth. *Sci. Monthly,* June:376-389.

Crick, F. H. C. and Watson, J. D. (1956). Structure of small viruses. *Nature,* 177:43-475.

Crick, F. H. C. and Watson, J. D. (1957). Virus structure: general principles. *CIBA Found. Symp. "The Nature of viruses",* pp. 5-13. Boston: Little, Brown

Dohner K. and Sodeik B. (2005). The role of the cytoskeleton during viral infection. *Curr. Top. Microbiol. Immunol.,* 285:67–108.

Drachenberg C. B., Papadimitriou J. C., Wali R., Cubitt C. and Ramos E. (2003). BK Polyoma virus allograft nephropathy: ultrastructural features from viral cell entry to lysis. *Am. J. Transplant.,* 3:1383–1392.

Dugan A., Eash S. and Atwood W. J. (2005). A N-linked glycoprotein with alpha(2,3)-linked sialic acid is a receptor of BK virus. *J. Virol.,* 79:14442–14445.

Eash S., Querbes W. and Atwood W. J. (2004). Infection of Vero cells by BK virus is dependent on caveolae. *J. Virol.,* 78:11583–11590.

Eash S. and Atwood W. J. (2005). Involvement of cytoskeletal components in BK virus infectious entry. *J. Virol.,* 79:11734–11741.

Finch, J. T., and Klug, A. (1959). Structure of poliomyelitis virus. *Nature,* 183:1709–1714.

Finch, J. T. and Klug, A. (1965). The structure of viruses of the papilloma-polyoma type: III. Structure of rabbit papilloma virus. *J. Mol. Biol.,* 13:1-12.

Fischer, M., Haase, I., Feicht, R., Richter, G., Gerhardt, S., Changeux, J. P., Huber, R. and Bacher, A. (2002). Biosynthesis of riboflavin 6,7-dimethyl-8-ribityllumazine synthase of *Schizosaccharomyces pombe*. *Eur. J. Biochem.,* 269:519-526.

Fischer, M., Haase, I., Kis, K., Meining, W., Ladenstein, R., Cushman, M., Schramek, N., Huber, R. and Bacher, A. (2003). Enzyme catalysis via control of activation entropy: Site-directed mutagenesis of 6,7-dimethyl-8-ribityl-lumazine synthase. *J. Mol. Biol.,* 326:783-793.

Fornasari MS, Laplagne DA, Frankel N, Cauerhff AA, Goldbaum FA and Echave J. (2004) Sequence determinants of quaternary structure in lumazine synthase. *Mol. Biol. Evol.,* 21:97-107.

Forstová, J., Krauzewicz, N., Sandig, V., Elliott, J., Palkova, Z., Strauss, M. and Griffin, B. E. (1995). Polyoma virus pseudocapsids as efficient carriers of heterologous DNA into mammalian cells. *Hum. Gene. Ther.,* 6:297-306.

Frisque, R. J., Bream, G. L. and Cannella, M. T. (1984). Human polyomavirus JC virus genom. *J. Virol.,* 51(2):458-469.

Gardner, S. D., Field, A. M., Coleman, D. V. and Hulme, D. (1971). New human papovavirus (B.K.) isolated from urine after renal transplantation. *Lancet.* 19;1 (7712):1253-7.

Gedvilaite, A., Frömmel, C., Sasnauskas, K., Micheel, B., Özel, M., Behrsing, O., Staniulis, J., Jandrig, B., Scherneck, S. and Ulrich, R. (2000). Formation of immunogenic virus-like particles by inserting epitopes into surface-exposed regions of Hamster polyomavirus major capsid protein. *Virology,* 273(1):21-35.

Gedvilaite, A., Zvirbliene, A., Staniulis, J., Sasnauskas, K., Krüger, D. H. and Ulrich, R. (2004). Segments of Puumala Hantavirus nucleocapsid protein inserted into chimeric polyomavirus-derived virus-like particles induce a strong immune response in mice. *Viral Immunol.,* 17(1):51–68

Gharakhanian, E., Sajo, A. K. and Weidman, M. K. (1995). SV40 VP1 assembles into disulfide-linked postpentameric complexes in cell-free lysates. *Virology,* 207:251-4.

Gleiter, S., and Lilie, H. (2001). Coupling of antibodies via protein Z on modified polyoma virus-like particles. *Protein Sci.,* 10(2):434-444.

Gleiter, S., and Lilie, H. (2003). Cell-type specific targeting and gene expression using a variant of polyoma VP1 virus-like particles. *Biol. Chem.,* 384(2):247-255.

Goldmann, C., Petry, H., Frye, S., Ast, O., Ebitsch, S., Jentsch, K-D., Kaup, F-J., Weber, F., Trebst, C., Nisslein, T., Hunsmann, G., Weber, T. and Luke, W. (1999). Molecular cloning and expression of major structural protein VP1 of the human polyomavirus JC virus: Formation of virus-like particles useful for immunological and therapeutic studies. *J. Virol.,* 73(5):4465-69.

Goldmann, C., Stolte, N., Nisslein, T., Hunsmann, G., Luke, W. and Petry, H. (2000). Packing of small molecules into VP1-virus-like particles of the human polyomavirus JC. *J. Virol. Meth.,* 90:85-90.

Griffith, J. P., Griffith, D. L., Rayment, I., Murakami, W. T. and Caspar, D. L. D. (1992). Inside polyomavirus at 25-Å resolution. *Nature,* 355:652-654.

Grimes JM, Burroughs JN, Gouet P, Diprose JM, Malby R, Zientara S, Mertens PP and Stuart DI. (1998). The atomic structure of the bluetongue virus core. *Nature,* 395:470-478.

Haase, I., Fischer, M., Bacher, A. and Schramek, N. (2003). Temperature-dependent presteady state kinetics o f Lumazine synthase from the hyperthermiophilic eubacterium *Aquifex aeolicus*. *J Biol Chem.,* 278:37909-37915

Haynes II, J. I., Chang, D. and Consigli, R. A. (1993). Mutations in the putative calcium-binding domain of polyomavirus VP1 affect capsid assembly. *J. Virol.,* 67(5):2486-95.

Henke, S., Rohmann, A., Bertling, W. M., Dingermann, Th. and Zimmer, Z. (2000). Enhanced in vitro oligonucleotide and plasmid DNA transport by VP1 virus-like particles. *Pharm. Research.,* 17(9):1062-2070.

Hom, L. and Volkman, L. E. (1998). Preventing proteolytic artefacts in the baculovirus expression system. *BioTechniques,* 25:18-20.

Hsu, C., Singh, P., Ochoa, W., Manayani, D. J., Manchester, M., Schneemann, A. and Reddy, V. S. (2006). Characterization of polymorphism displayed by the coat protein mutants of tomato bushy stunt virus. *Virol.,* In press.

Imperiale M. J. (2001). Human polyomaviruses: molecular and clinical perspectives. In: The Human Polyomaviruses: An Overview, vol. pp. 53–71, Khalili K. and Stoner G. L. (eds.), Wiley-Liss, New York.

Ishizu, KI., Watanabe, H., Han, SI., Kanesashi, SN., Hoque, M., Yajima, H., Kataoka, K. and Handa, H. (2001). Roles of disulfide linkage and calcium ion-mediated interactions in assembly and disassembly of virus-like particles composed of simian virus 40 VP1 capsid protein. *J. Virol.,* 75(1):61-72.

Jao, C. C., Weidman, M. K., Perez, A. R. and Gharakhanian, E. (1999). Cys9, Cys104 and Cys207 of simian virus 40 VP1 are essential for inter-pentamer disulfide-linkage and stabilization in cell-free lysates. *J. Gen. Virol.,* 80:2481-89.

Jones, T.A., Zou, J.Y., Cowan, S.W. and Kjeldgaard, M. (1991). Improved methods for building protein models in electron density maps and the location of errors in these models. *Acta Cryst* A47, 110-119.

Jones, S. and Thornton, J. M. (1996). Principles of protein-protein interactions. *Proc. Natl. Acad. Sci. USA,* 93:13-20.

Kanesashi, SN., Ishizu, KI., Kawano, MA., Han, SI., Tomita, S., Watanabe, H., Kataoka, K. and Handa, H. (2003). Simian virus 40 VP1 capsid protein forms polymorphic assemblies in vitro. *J. Gen. Virol.,* 84:1899-1905.

Karas M. and Hillenkamp F. (1988). Laser desorption ionization of proteins with molecular mass exceeding 10,000 Daltons. *Anal. Chem.*, 60:2299-2301.

Kasamatsu H. and Nakanishi A. (1998). How do animal DNA viruses get to the nucleus? *Annu. Rev. Microbiol.,* 52:627–686.

Kellenberger, E. (1969). Polymorphic assemblies of the same major virus protein subunit. *In* Engström, A. and Strandberg B. (ed.), Nobel Symp. Symmetry and Function of Biological Systems at the Macromolecular Level, 11th, Almqvist and Wiksell Förlag AB, Stockholm (Wiley, New York), pp. 425-436.

Kis, K., Volk, R. and Bacher, A. (1995). Biosynthesis of Riboflavin. Studies on the reaction mechanism of 6,7-dimethyl-8-ribityllumazine synthase. *Biochemistry,* 34:2883-2892.

Kis, K., Kugelbrey, K. and Bacher, A. (2001). Biosynthesis of riboflavin. The reaction catalyzed by 6,7-dimethyl-8-ribityllumazine synthase can proceed without enzymatic catalysis under physiological conditions. *J. Org. Chem.,* 66:2555-2559.

Kiselev, N. A. and Klug, A. (1969). The structure of the papilloma-polyoma type: V. Tubular variants built of pentamers. *J. Mol. Biol.,* 40:155-171.

Klug, A. (1969). Point groups and the design of aggregates. *In* Engström, A. and Strandberg B. (ed.), Nobel Symp. Symmetry and Function of Biological Systems at the Macromolecular Level, 11th, Almqvist och Wiksell Förlag AB, Stockholm (Wiley, New York), pp. 425-436.

Klug, A., and Finch, J. T. (1960). The symmetries of the protein and nucleic acid in turnip yellow mosaic virus: X-ray diffraction studies. *J. Mol. Biol.* 2:201–215.

Krauzewicz, N., Stokrová, J., Jenkins, C., Elliott, M., Higgins CF, and Griffin, BE. (2000). Virus-like gene transfer into cells mediated by polyoma virus pseudocapsids. *Gene. Ther.,* 7:2122-2131.

Krol, M. A., Olson, N. H., Tate, J., Johnson, J. E., Baker, S. B. and Ahlquist, P. (1999). RNA-controlled polymorphism in the in vivo assembly of 180-subunit

and 120-subunit virions form a single capsid protein. *Proc. Natl. Acad. Sci. USA,* 96(24):13650-13655.

Kurland CG. (1992). Translational accuracy and the tness of bacteria. *Annu. Rev. Genet.,* 26:29-50.

Ladenstein, R., Meyer, B., Huber, R., Labischinski, H., Bartels, K., Bartunik, H., Bachmann, S., Ludwig, H. C. and Bacher, A. (1986). Heavy Riboflavin synthases from *Bacillus subtilis*: Particle dimensions, crystal packing and molecular symmetry. *J. Mol. Biol.,* 187:87-100.

Ladenstein R, Bacher A and Huber R. (1987). Some observations of a correlation between the symmetry of large heavy-atom complexes and their binding sites on proteins. *J. Mol. Biol.,* 195:751-753.

Ladenstein, R., Schneider, M., Huber, R,. Bartunik, H.-D., Wilson, K., Schott, K. and Bacher, A. (1988). Heavy Riboflavin synthases from *Bacillus subtilis,* Crystal structure analysis of the icosahedral β_{60} capsid at 3.3 Å resolution. *J. Biol. Chem.,* 203:1045-1070.

Ladenstein, R., Meining, W., Zhang, X., Fischer, M. and Bacher, A. 2004. Metamorphsis of and enzyme, p. 198-221. *In* R. H. Cheng and L. Hammar (ed.), Conformational proteomics of macromolecular architecture. World Scientific publishing Co. Pte. Ltd. Singapore.

Laemmli, U. K. (1970). Cleavage of structural proteins during the assembly of the head of Bacteriophage T4. *Nature,* 227:680-685.

Larsen, T. A., Olson, A. J. and Goodsell, D. S. (1998). Morphology of protein-protein interfaces. *Structure,* 6:421-427.

Lee, J., Gibson, B. G., O'Kane, D. J., Kohnle, A. and Bacher, A. (1992). Fluorescence study of the ligand stereospecificity for binding to lumazine protein. *European Journal of Biochemistry.* 210:711-719.

Li, P. P., Nakanishi, A., Clark, S. W. and Kasamatsu, H. (2002). Formation of transitory intrachain and interchain disulfide bonds accompanies the folding and oligomerization of simian virus 40 vp1 in the cytoplasm. *Proc. Natl. Acad. Sci. USA,* 99(3):1353-1358.

Li, P. P., Nakanishi, A., Tran, M. A., Ishizu, KI., Kawano, M., Phillips, M., Handa, H., Liddington, R. C. and Kasamatsu, H. (2003). Importance of VP1 calcium-binding residues in assembly, cell entry, and nuclear entry of SV40. *J. Virol.,* 77(13):7527-7538.

Li, TC., Takeda, N., Kato, K., Nilsson, J., Xing, L., Haag, L., Cheng, R. H. and Miyamura T. (2003). Characterization of Self-Assembled Virus-like Particles of Human Polyomavirus BK Generated by Recombinant Baculoviruses. *Virology,* 311:115–124.

Liddington, R. C., Yan, Y., Moulai, J., Sahli, R., Benjamin, T. L., and Harrison, S. C. (1991). Structure of simian virus 40 at 3.8-A resolution. *Nature,* 354**:**278-284.

Liljas, L. 2004. The role of disordered segments in viral coat proteins, p. 53-77. *In* R. H. Cheng and L. Hammar (ed.), Conformational proteomics of macromolecular architecture. World Scientific publishing Co. Pte. Ltd. Singapore.

Lo Conte, L., Chothia, C. and Janin, J. (1999). The atomic structure of protein-protein recognition sites. *J. Mol. Biol.,* 285:2177-2198.

Lu G, Zhou ZH, Baker ML, Jakana J, Cai D, Wei X, Chen S, Gu X and Chiu W. (1998). Structure of double-shelled rice dwarf virus. *J. Virol.,* 72:8541-8549.

Ludwig HC, Lottspeich F, Henschen A, Ladenstein R and Bacher A. (1987). Heavy riboflavin synthase of Bacillus subtilis. Primary structure of the β subunit. *Journal of Biological Chemistry,* 262:1016-1021.

Mattern, C. F. T., Takemoto, K. K. and DeLeva, A. M. (1967). Electron microscopic observations on multiple polyoma virus-related particles. *Virology,* 32:378-392.

May, T., Gleiter, S. and Lilie, H. (2002). Assessment of cell type specific gene transfer of polyoma virus like particles presenting a tumor specific antibody Fv fragment. *J. Virol. Methods,* 105(1):147-157.

Meining, W., Mörtl, S., Fischer, M., Cushman, M., Bacher, A. and Ladenstein, R. (2000). The atomic structure of pentameric Lumazine synthase from *Saccharomyces cerevisiae* at 1.85 Å resolution reveals the binding mode of a phosphonate intermediate analogue. *J. Mol. Biol.,* 299:181-197.

Monod, J. (1969). On symmetry and function in biological systems, pp. 15-29. *In* Engström, A. and Strandberg B. (ed.), Nobel Symp. Symmetry and Function of Biological Systems at the Macromolecular Level, 11th, Almqvist and Wiksell Förlag AB, Stockholm (Wiley, New York).

Morgan, G. J. 2004. Early theories of virus structure, p. 3-40. *In* R. H. Cheng and L. Hammar (ed.), Conformational proteomics of macromolecular architecture. World Scientific publishing Co. Pte. Ltd. Singapore.

Morgunova, E., Meining, W., Illarionov, B., Haase, I., Jin, G., Bacher, A., Cushman, M., Fischer, M. & Ladenstein, R. (2005). Crystal structure of lumazine synthase from Mycobacterium tuberculosis as a target for rational drug design: binding mode of a new class of purinetrione inhibitors. *Biochemistry,* 44:2746-58.

Naitow H, Tang J, Canady M, Wickner RB and Johnson JE. (2002) L-A virus at 3.4 A resolution reveals particle architecture and mRNA decapping mechanism. *Nat. Struct. Biol.,* 9:725-728.

Nakagawa A, Miyazaki N, Taka J, Naitow H, Ogawa A, Fujimoto Z, Mizuno H, Higashi T, Watanabe Y, Omura T, Cheng RH and Tsukihara T. (2003) The atomic structure of rice dwarf virus reveals the self-assembly mechanism of component proteins. *Structure (Camb),* 11:1227-1238.

Nakanishi A., Clever J., Yamada M., Li P. P. and Kasamatsu H. (1996). Association with capsid proteins promotes nuclear targeting of simian virus 40 DNA. *Proc. Natl. Acad. Sci. USA,* 93:96–100.

Nilsson, J., Miyazaki, N., Xing, L., Wu, B., Hammar, L., Li, TC., Takeda, N., Miyamura T. and Cheng, R. H. (2005). Structure and Assembly of a *T*=1 Virus-like Particle in BK Polyomavirus. *J. Virol.*, 79(9):5337-5345.

Otto, M. K. and Bacher, A. (1981). Ligand-binding studies on light riboflavin synthase from *Bacillus subtilis*. *European Journal of Biochemistry,* 115:511-517.

Ou, WC., Wang, M., Fung, CY., Tsai, RT., Chao, PC., Hseu, TH. and Chang, D. (1999). The major capsid protein, VP1, of human JC virus expressed in *Escherichia coli* is able to self-assemble into a capsid-like particle and deliver exogenous DNA into human kidney cells. *J. Gen. Virol.,* 80:39-46.

Ou, WC., Chen, LH., Wang, M., Hseu, TH. and Chang, D. (2001). Analysis of minimal sequences on JC virus VP1 required for capsid assembly. *J. Neuro Virology,* 7:298-301.

Parker J. (1989). Errors and alternatives in reading the universal genetic cod. *Microbiol. Rev.,* 53:273-298.

Persson, K., Schneider, G., Jordan, D. B., Viitanen, P. V. And Sandalova. T. (1999). Crystal structure of a pentameric fungal and an icosahedral plant lumazine

synthase reveals the structural basis for differences in assembly. *Protein Science,* 8:2355-2365.

Rayment, I., Baker, T. S., Caspar, D. L. D. and Murakami, W. T. (1982). Polyoma virus capsid structure at 22.5 Å resolution. *Nature,* 295:110-115.

Rodgers, R. E. D., Chang, D., Cai, X. and Consigli, R. A. (1994). Purification of recombinant budgerigar fledgling disease virus VP1 capsid protein and its ability for in vitro capsid assembly. *J. Virol.,* 68(5):3386-3390.

Rossmann MG. (2000). Fitting atomic models into electron-microscopy maps. *Acta Crystallogr D,* 56:1341-1349.

Salunke, D. M., Caspar, D. L., and Garcea, R. L. (1986). Self-assembly of purified polyomavirus capsid protein VP1. *Cell.,* 46:895-904.

Salunke, D. M., Caspar, D. L. D. and Garcea, R. L. (1989). Polymorphism in the assembly of polyomavirus capsid protein VP1. *Biophys. J.,* 56:887-900.

Sandalon, Z., Dalyot-Herman, N., Oppenheim, A. B. and Oppenheim, A. (1997). In vitro assembly of SV40 virions and pseudovirions: vector development for gene therapy. *Hum. Gene. Ther.,* 8:843-849.

Sangita, V., Lokesh, G. L., Satheshkumar, P. S., Vijay, C. S., Saravanan, V., Savithri, H. S. and Murthy, M. R. N. (2004). *T*=1 capsid structures of *Sesbania* mosaic virus coat protein mutants: Determinants of *T*=3 and *T*=1 capsid assembly. *J. Mol. Biol.,* 342:987-999.

Savithri, H. S. and Erickson, J. W. (1983). The self-assembly of the Cowpea strain of Southern bean mosaic virus: Formation of *T*=1 and *T*=3 nucleoprotein particles. *Virol.,* 126:328-335.

Scheuring, J., Kugelbrey, K., Weinkauf, S., Cushman, M., Bacher, A. and Fischer, M. (2001). ^{19}F NMR ligand perturbation studies on 6,7-Bis(trifluoromethyl)-8-ribityllumazine-7-hydrates and the lumazine synthase complex of *Bacillus subtilis*. Site-directed mutagenesis changes the mechanism and the stereoselectivity of the catalyzed haloform-type reaction. *J. Org. Chem.,* 66:3811-3819.

Schmidt, U., Rudolph, R. and Böhm, G. (2000). Mechanism of assembly of recombinant murine polyomavirus-like particles. *J. Virol.,* 74(4):1658-1662.

Schramek, N., Haase, I., Fischer, M. and Bacher, A. (2003). Biosynthesis of riboflavin. Single turnover kinetic analysis of 6,7-dimethyl-8-ribityllumazine synthase. *J. Am. Chem. Soc.,* 125:4460-4466.

Schwede, T., J. Kopp, N. Guex, and M. C. Peitsch. (2003). SWISS-MODEL: and automated protein homology-modeling server. *Nucleic Acids Res.,* 31:3381–3385.

Sciutto, E., Toledo, A., Cruz, C., Rosas, G., Meneses, G., Laplagne, D., Ainciart, N., Cervantes, J., Fragoso, G. and Goldbaum, F. A. (2005). *Brucella* spp. Lumazine synthase: a novel antigen delivery system. *Vaccine*, 23:2784-2790.

Seebeck, F. P., Woycechowsky, K. J., Zhuang, W., Rabe, J. P. and Hilvert, D. (2006). A simple tagging system for protein encapsulation. *J. Am. Chem. Soc.,* 128:4516-4517.

Srere PA. (1984). Why are enzymes so big? *Trends Biochem. Sci.*, 9:387-390.

Stehle, T., Yan, Y., Benjamin, T. L. And Harrison, S. C. (1994). Structure of murine polyomavirus complexed with an oligosaccharide receptor fragment. *Nature*, 369:160-163.

Stehle, T., Gamblin, S. J., Yan, Y., and Harrison, S. C. (1996). The structure of simian virus 40 refined at 3.1 Å resolution. *Structure.,* 4:165-182.

Stites, W. E. (1997). Protein-protein interactions: Interface structure, binding thermodynamics, and mutational analysis. *Chem. Rev.,* 97:1233-1250.

Stubenrauch, K., Gleiter, S., Brinkmann, U., Rudolph, R. and Lilie, H. (2001). Conjugation of an antibody Fv fragment to a virus coat protein: cell-specific targeting of recombinant polyoma-virus-like particles. *Biochem. J.,* 356(Pt 3):867-873.

Tanaka K., Waki H., Ido Y., Akita S., Yoshida Y. and Yoshida T. (1988). Protein and polymer analysis up to m/z 100,000 by laser ionization time-of-flight mass spectrometry. *Rapid Commun. Mass Spectrom.*, 2:151-153

Tang, J., Johnson, J. M., Dryden, K. A., Young, M. J., Zlotnick, A. and Johnson, J. E. (2006). The role of subunit hinges and molecular "switches" in the control of viral capsid polymorphism. *J. Struct. Biol.,* 154:59-67.

Tegerstedt, K., Lindencrona, J. A., Curcio, C., Andreasson, K., Tullus, C., Forni, G., Dalianis, T., Kiessling, R. and Ramqvist, T. (2005). A single vaccination with polyomavirus VP1/VP2Her2 virus-like particles prevents outgrowth of HER-2 / neu-expression tumors. *Cancer Res.,* 65(13):5953-5957.

Tegerstedt, K, Franzén, A. V., Andreasson, K., Joneberg, J., Heidari, S., Ramqvist, T. and Dalianis, T. (2005). Murine polyomavirus virus-like particles (VLPs) as vectors for gene and immune therapy and vaccines against viral infections and cancer. *Anticancer Res.,* 25(4):2601-2608.

Thuman-Commike, P. A., Greene, B., Malinski, J. A., King, J., and Chiu, W. (1998). Role of the Scaffolding Protein in P22 Procapsid Size Determination Suggested by $T = 4$ and $T = 7$ Procapsid Structures. *Biophys. J.,* 74(1):559–568

Touzé, A., Bousarghin, L., Ster, C., Combita, AL., Roingeard, P. and Coursaget, P. (2001). Gene transfer using polyomavirus BK virus-like particles expressed in insect cells. *J. Gen. Virol.,* 82:3005-3009.

Walker, D. L., and Frisque, R. J. (1986). The biology and molecular biology of JC virus. *In* "The papovaviridae" (N. P. Salzman, Ed.), Vol. 1, pp. 161-193. Plenum press, New York.

Walter, G. and Deppert, W. (1975). Intermolecular disulfide bonds: An important structural feature of the polyoma virus capsid. *Cold spring Harbor symp. Quant. Biol.,* 39:255-257.

Wang, M., Tsou, T-H., Chen, L-S., Ou, W-C., Chen, P-L., Chang, C-F., Fung, C-Y. and Chang, D. (2005). Inhibition of simian virus 40 large tumor antigen expression in human fetal glial cells by an antisense oligodeoxynucleotide delivered by the JC virus-like particle. *Human Gene Therapy.,* 15:1077-1090.

Wildy, P., Russell, W. C. and Horne, R. W. (1960). The morphology of herpes virus. *Virology,* 12:204-222.

Wu B, Hammar L, Xing L, Markarian S, Yan J, Iwasaki K, Fujiyoshi Y, Omura T and Cheng RH. (2000). Phytoreovirus T = 1 core plays critical roles in organizing the outer capsid of T = 13 quasi-equivalence. *Virology,* 271:18-25.

Yan, Y., Stehle, T., Liddington, R. C., Zhao, H. and Harrison, S. C. (1996). Structure determination of simian virus 40 and murine polyomavirus by a combination of 30-fold and 5-fold electron-density averaging. *Structure*, 4:157-164.

Yang, YW. and Chen, LH. (2000). Gene delivery via polyomavirus major capsid protein VP1 isolated from recombinant E. coli. *Biotechnol. Appl. Biochem.,* 32:73-79.

Zhang, X., Meining, W., Fischer, M., Bacher, A. and Ladenstein, R. (2001). X-ray structure analysis and crystallographic refinement of Lumazine synthase from the hyperthermophile *Aquifex aeolicus* at 1.6 Å resolution: Determinants of thermostability revealed from structural comparisons. *J. Mol. Biol.,* 306:1099-1114.

Zhang, X., Meining, W., Cushman, M., Haase, I., Fischer, M., Bacher, A. and Ladenstein, R. (2003). A Structure-based model of the reaction catalyzed by lumazine synthase from *Aquifex aeolicus*. *J. Mol. Biol.,* 328:167-182.

Zylberman V, Craig PO, Klinke S, Braden BC, Cauerhff A and Goldbaum FA. (2004). High order quaternary arrangement confers increased structural stability to Brucella sp. lumazine synthase. *J. Biol. Chem.,* 279:8093-8101.